VENTILATION FOR WORK IN CONFINED SPACES

Richard P. Garrison, Ph.D., CIH, CSP

Principal Investigator and
Associate Professor of Industrial Health

School of Public Health
The University of Michigan
Ann Arbor, MI 48109

Final Report to the
National Institute of Occupational Safety and Health
Washington, D.C.

Project No. 5 R01-OH02329

March 27, 1991

50272-101

REPORT DOCUMENTATION PAGE	1. REPORT NO.	2.	3. PB92-108455

4. Title and Subtitle: Ventilation for Work in Confined Spaces

5. Report Date: 1991/03/27

6.

7. Author(s): Garrison, R. P.

8. Performing Organization Rept. No.

9. Performing Organization Name and Address: School of Public Health, The University of Michigan, Ann Arbor, Michigan

10. Project/Task/Work Unit No.

11. Contract (C) or Grant(G) No.
(C)
(G) R01-OH-02329

12. Sponsoring Organization Name and Address

13. Type of Report & Period Covered

14.

15. Supplementary Notes

16. Abstract (Limit: 200 words) A series of studies was conducted involving experimental testing and computer modeling to evaluate ventilation characteristics and improve design methods for confined spaces (CS). The models were developed in an effort to predict CS ventilation effectiveness and to advance ventilation design technology. Multicellular models of CS ventilation were programmed and tested for two basic variations. Model 1 used experimental data and approximations to represent airflow in the CS. Model 2 used airflow characteristics predicted by another computer model. Mechanical ventilation was far more effective than natural ventilation could have been in CS. In general supply ventilation was more effective than exhaust ventilation. The inlet/outlet elevation had a significant effect on effectiveness with low inlet/outlet elevations being generally more effective in diluting contaminants. Ventilation time decreased with increasing flow rate, but not usually in a linear manner. Significant, variable, and somewhat inconsistent effects on ventilation time were observed by changing the CS model shape. Ventilation effectiveness characteristics varied significantly with contaminant stratification caused by heavier than air contaminants. Dilution ventilation characteristics for simulated toxic concentrations were similar to those for oxygen deficiency caused by nitrogen (7727379).

17. Document Analysis a. Descriptors

b. Identifiers/Open-Ended Terms: NIOSH-Publication, NIOSH-Grant, Grant-Number-R01-OH-02329, Tunneling, End-Date-12-31-1990, Control-technology, Ventilation-systems, Confined-spaces, Air-quality-control, Air-quality-monitoring, Sewer-cleaning, Miners

c. COSATI Field/Group

18. Availability Statement

19. Security Class (This Report)

21. No. of Pages: 74

22. Security Class (This Page)

22. Price

Table of Contents

List of Tables

List of Figures

List of Significant Findings

1. Mechanical ventilation was effective in eliminating oxygen deficiency in a variety of confined space (CS) model, ventilation, and contaminant situations. It was much more effective than natural (non-mechanical) ventilation could have been.

2. Supply ventilation was generally more effective than was exhaust ventilation. CS locations aligned with the supply outlet experienced very rapid oxygen recovery, much faster than for non-aligned CS locations.

3. Inlet/outlet (I/O) elevation had significant effects upon ventilation effectiveness. Low I/O elevations were generally more effective in diluting contaminants than were higher elevations.

4. Ventilation time decreased with increasing flow rate, but not usually in a simple linear manner. Sometimes there were limits above which increasing ventilation flow rate had relatively little effect.

5. Changes in CS model shape had significant, variable, and somewhat inconsistent effects upon ventilation time, depending primarily upon whether contaminants were significantly heavier-than-air.

6. Geometric similarity and equal nondimensional flow rate (ACH) were necessary and sufficient for two cubical CS models of different size to demonstrate very similar ventilation characteristics.

7. Ventilation effectiveness (oxygen recovery) characteristics varied significantly with contaminant stratification caused by heavier-than-air (HTA) contaminants. Oxygen recovery was slower for increasing contaminant density. Neutrally-buoyant nitrogen was not a good predictor of ventilation characteristics for HTA contaminants.

8. Dilution ventilation characteristics for simulated toxic concentrations were similar to those for oxygen deficiency caused by nitrogen. This may broaden the potential usefullness of the empirical database from these studies of oxygen recovery.

9. A multicellular contaminant dispersion computer model was able to predict dilution ventilation effectiveness reasonably well for situations involving purging, continuous release, and variable rates of contaminant release.

10. The Boundary Element Method (BEM) provided reasonably good predictions of velocity characteristics for the multicellular model in the case of exhaust ventilation. BEM predictions were not as good for supply ventilation.

Abstract

This is a report on findings from a series of studies involving experimental testing and computer modeling to evaluate ventilation characteristics and to improve design methods for confined spaces (CS). Confined spaces are the sites of many tragic accidents and deaths. Airborne contaminants are the leading cause of CS deaths. Mechanical ventilation is a primary means for controlling air contaminant hazards. Unfortunately, there are very few design guidelines or established criteria for CS ventilation. These studies address this need for more information.

Hazardous CS atmospheres can involve oxygen deficiency and/or the presence of toxic and possibly flammable vapor and gases. These studies have investigated several configurations of laboratory CS models. The basic CS model was cubical with a single opening in the top corner. Several noncubical variations in CS model shape were tested. Mechanical ventilation was introduced to the CS models through the top opening in two modes -- exhaust and supply -- at measured flow rates (ACH, "air changes" per hour) and at specific inlet/outlet elevations (%H, fraction of CS model height). Oxygen deficiency was caused by test contaminant gases of different density, ranging from neutrally-buoyant N_2 to very heavy SF_6; specifically -- N_2, CO_2, HC22 (a "Freon"), and SF_6 (specific gravities of 0.98, 1.5, 3.0, and 5.05, respectively). Much lower contaminant concentrations were also tested, simulating (using isobutylene) levels of potentially toxic gases/vapors. These results were compared to findings for O_2 deficiency caused by N_2. Experimental data were collected at four locations, most often at different CS model elevations. The experimental data were regressed against a simple exponential model for O_2 recovery from an initial deficiency. This provided an empirical database which represents the experimental data quite accurately. Findings from the experimental studies of CS models suggest guidelines for designing CS ventilation to accomplish O_2 recovery and the reduction of airborne toxic contaminants.

Computer models were developed in an effort to predict CS ventilation effectiveness (contaminant dispersion and dilution) and to advance ventilation design technology. Multicellular models of CS ventilation were programmed and tested for two basic variations: Model 1 using experimental data and approximations to represent airflow in the CS, and Model 2 using airflow characteristics predicted by another computer model. The airflow model for multicellular Model 2 applied numerical procedures known as the Boundary Element Method (BEM). Models 1 and 2 predicted O_2 recovery characteristics reasonably well, but not yet well enough to serve as useful tools for CS ventilation design.

Introduction

Ventilation is an extremely important engineering control measure for atmospheric contaminants which present real and potential hazards for work conducted in confined spaces (CS). There are many complex issues associated with ventilation design for confined spaces, and there are presently very few specific guidelines, standards, or other criteria which can be used.[1]

Each year, in the United States, roughly 200-300 persons die in confined space accidents.[2,3] Atmospheric contaminants are the leading cause of accidents leading to death and serious injury in confined spaces. This underscores the importance of ventilation, which many times is the only method available to reduce contaminant concentrations for CS entries. Administrative controls for CS entries reduce risk but do not alter hazardous conditions.

There are many important issues for programs to manage safe CS entries.[4,5] Ventilation is one of the most important issues. Other important issues include monitoring for airborne contaminants prior to and during entry, utilizing written permits, providing entry attendants, developing emergency procedures, training, and having specific written policy and entry procedures. This report is intended to emphasize the importance of mechanical ventilation as a primary means to control airborne CS hazards. It does not mean to suggest that ventilation is necessarily more important than other control measures.

Very few field or laboratory studies have been conducted on CS ventilation effects. One field study, conducted about thirty years ago, investigated ventilation design considerations for welding operations inside refinery processing towers.[6] Another field study, conducted last year, investigated air contaminants and oxygen levels in waste-water manholes.[7] Unfortunately, there is very little else available in the literature. There is a clear need for studies to help establish guidelines, possibly standards, and to otherwise help design effective ventilation for contaminant control in confined spaces.

NIOSH (the National Institute for Occupational Safety and Health) has studied CS entry issues. A "Criteria Document" on recommendations for working in confined spaces was published in 1979.[8] This study and report recognized that ventilation is important, but did not emphasize ventilation or provide any specific information on how to accomplish "adequate ventilation" for CS atmospheric hazards. In another report, NIOSH offered one of the very few specific recommendations in published literature pertaining to CS

ventilation design; it recommends a ventilation volume flow rate of at least 20 "air changes" per hour.[9]

OSHA (the Occupational Safety and Health Administration) has developed what is currently a proposed standard for "Permit Entry Confined Spaces."[10] This proposed standard does not emphasize ventilation as a primary means of engineering control for CS entries. It has very few provisions which even mention ventilation.[11,12]

ANSI (the American National Standards Institute) has recently revised its guidelines on safety for confined spaces.[13] The current (recently revised) guidelines place significant emphasis on preventing atmospheric hazards, with greater emphasis on ventilation than in previous ANSI guidelines. However, there are no specific ANSI design criteria offered for CS ventilation. The ACGIH (American Conference of Governmental Industrial Hygienists) "Ventilation Manual,"[14] although uniquely useful for many design problems, contains no specific guidelines on ventilation for confined spaces.

This report presents findings from a series of laboratory studies conducted on CS ventilation effects. Three studies investigated effects related to recovery from oxygen deficiency in CS models.[15,16,17] One study measured and evaluated contaminant reduction effects at much lower concentrations, simulating toxic airborne substances.[18] Two studies investigated mathematical modeling methods for predicting CS ventilation effects.[19,20] These studies were supported by a research grant from NIOSH.

Experimental Facilities and Methods

Figures 1 through 6 illustrate the experimental facilities. The principal components, illustrated in Figure 1, were the CS models and the ventilation, contaminant release, air sampling, and analytical systems. The CS models for this study were of several cubical and noncubical configurations. A cube was selected as the basic CS model shape because it is the simplest geometric shape and favors systematic variations into noncubical shapes. A cube is also representative of many actual confined spaces, e.g., vaults, tanks, and process equipment.

The ventilation system consisted of a centrifugal blower, inlet/outlet piping and valves, an orifice-plate flow meter, and plastic pipe (duct) running into the CS models with removable end sections of different lengths. The plastic pipe had a nominal inside diameter of 5.1 cm (2 inches) and an outside diameter of 6.1 cm (2.4 inches). Valve operation allowed selection of exhaust or supply air flow and control of volume flow rate

to the CS models. Volume flow rate was measured in dimensionless units of volumetric flow, "air changes" per hour (ACH = ventilation flow in 1 hour/CS model volume).

Several contaminant gases were used for the experimental testing. They were released from pressurized cylinders into the bottom of a CS model to create an oxygen-deficient atmosphere. Each experimental test began with the establishment of a specific test atmosphere. Most of the test atmospheres were made by introducing contaminant in an amount equal to one half (50%) of the CS model volume. Each test run began (measured time = 0) when the ventilation system was turned "on."

Samples of air were taken at four locations inside the CS models. The samples were drawn from a manifold connected to the inlet of a small diaphragm pump. Each sampling line consisted of rigid tubing inside the CS model, a bulkhead fitting in the model wall, and flexible tubing to a flowmeter, oxygen sensor, and the suction manifold. Equal sampling flow rates (approximately 0.25 L/min) were maintained in each line.

The analytical system utilized four electrochemical oxygen sensors, one in each sampling line, connected to a four-channel monitor (ENMET Corporation). The sensors responded to the partial pressure of oxygen in the air and provided linear response over a broad range of oxygen concentration. Analog voltage signals from the sensors were converted to digital data, read by a personal computer, displayed on the computer monitor, and stored on diskettes. Data were collected continuously for each test, with one measurement approximately every second for each sampling location until oxygen recovery was very nearly complete (within 0.1 $\%O_2$ of ambient).

Figure 1 illustrates a portion of the experimental facility as it was used for the study of simulated toxic concentrations, much lower than concentrations causing oxygen deficiency. The cubical CS model configuration, ventilation system, and sampling locations were the same as were used for oxygen deficiency.

Isobutylene (IBE) was selected to simulate toxic concentrations because it was safe to use and relatively easy to monitor. It was supplied through the bottom of the CS model from a cylinder containing a 1.0 % mixture (10,000 ppm) of IBE in air. IBE concentrations were measured with a photoionization detector (PID). The PID was used with a portable gas chromatograph (Thermo Electron Instruments, Model 511A), although a separation column was not used because no contaminant separation was needed. Analog signals from the PID were converted to digital data and recorded on a personal computer.

A multiple-point sampling system was used because there was only one PID. This system utilized four three-way solenoid valves which were activated by relays controlled by the computer. A purge pump was used to maintain fresh samples at each solenoid. Another pump was used to draw samples at a rate of 200 ml per minute from the solenoids to the PID. The sampling system measured IBE concentration every ten seconds (i.e., every 40 seconds at each of the 4 sampling locations).

Several different initial concentrations (C_0) of IBE were tested -- 100, 350, 700, and 1400 ppm -- encompassing a range representative of toxic contaminant hazards. A test run involved setting up the desired ventilation parameters, establishing the initial IBE concentration in the CS model, starting the ventilation system, recording IBE concentration (ppm) as a function of time, and terminating the test when the IBE concentration had fallen to about 1 % of its initial value.

Figure 2 illustrates the CS models which were studied. All of these CS models were tested with nitrogen. Three were tested, with some variations, for the HTA contaminants. CS Models A and B were cubical. CS Model A, measuring 0.61 m (2.0 ft) on each edge, was the basic model and was the most thoroughly studied. The overall dimensions of CS Model B were twice those of CS Model A, with a volume eight-times greater. CS Model B was an expansion of the basic CS Model A in three directions. Five noncubical CS models (C, D1, D2, E1, and E2) also were investigated.

CS Model C had the same height 0.61 m (2.0 ft), as the basic cube (CS Model A), with twice the width and length, 1.22 m (4.0 ft). CS Model C was, in effect, the top half of CS Model B and represented two-directional sideways (perpendicular to the ventilation axis) expansion from the basic CS Model A.

CS Models D1 and D2 were the same CS model, but they had different ventilation configurations. The D models had twice the volume of CS Model A. CS Model D1 involved sideways (horizontal) expansion from CS Model A, with the vertical ventilation axis parallel to the short sides of the model, measuring 0.61 m (2.0 ft). CS Model D2 was configured vertically, representing depthwise expansion from CS Model A, with the ventilation axis parallel to the long sides of the model measuring 1.22 m (4.0 ft).

CS Models E1 and E2 also were the same model except for the orientation of the ventilation axis. The E models had three times the volume of CS Model A. CS Model E1 involved sideways expansion from CS Model A and was configured with the vertical axis of the ventilation outlet parallel to the short sides. CS Model E2 involved depthwise

expansion from CS Model A and was configured with the ventilation axis parallel to the long sides, measuring 1.83 m (6.0 ft).

The CS models for the nitrogen (causing O_2 deficiency) studies were selected to provide several comparisons of model shape characteristics.

- o CS Model A vs. B -- three-directional (vertical and horizontal) expansion from the basic cube (8 times more volume).
- o CS Model A vs. C -- two-directional sideways (horizontal) expansion from the basic cube (4 times more volume).
- o CS Model A vs. D1 vs. E1 -- one-directional sideways (horizontal) expansion from the basic cube (2 and 3 times more volume).
- o CS Model A vs. D2 vs. E2 -- one-directional depthwise (vertical) expansion from the basic cube (2 and 3 times more volume).

The CS models were constructed of plywood on their top, bottom, and two sides, with clear plexiglas on the other two sides. The interior wooden surfaces were painted black. The size and position of the circular top opening was the same for all of the CS model shapes, i.e., 15.2 cm (6.0 inches) in diameter and centered in a corner, 15.2 cm (6.0 inches) from each of the two closest walls of the model. The inside diameter of the ventilation pipe, 5.1 cm (2.0 inches), was the same for all of these models. A different construction of the basic cubical CS Model A was used for the IBE testing. This model had the same cubical size. It used an angle-iron frame to mount wooden panels forming the top, bottom, and three sides. The front panel was made of clear plexiglas.

The four sampling locations were set at the same non-dimensional positions for all of the CS model testing with N_2 causing O_2 deficiency.

- o Location 1 was the lowest, at 15% of model height from the bottom (15 %H), centered in the vertical quadrant containing the ventilation pipe.
- o Locations 2 and 3 were diagonally opposed to each other, at the mid plane (50 %H) and centered in quadrants adjacent to that of Location 1.
- o Location 4 was diagonally opposed to Location 1, at an elevation of 85% of model height (85 %H).

The experimental methods for the heavier-than-air (HTA) contaminants were different from those of the nitrogen studies in several important ways.

- o Contaminants other than N_2 -- specifically, the HTA gases of carbon dioxide (CO_2), halocarbon-22 (chlorodifluoromethane, HC22), and sulfur hexaflouride (SF_6) were tested. The test gases were selected on the bases of specific gravity and low hazard potential. They were introduced slowly at the bottom of the CS models to

minimize dispersion prior to ventilation testing.

- o Different sampling locations -- with HTA contaminants, it was necessary to place greater emphasis on effects at different elevations inside the CS model. For this study, samples were taken at four elevations on the vertical central axis. In the nitrogen studies, the sampling locations were in different vertical quadrants of the CS models.
- o Limited CS model configurations -- in order to have a manageable number of tests, it was necessary to reduce the number of CS model shapes and sizes and the variations of ventilation design parameters.

Figure 3 illustrates the CS model shapes, ventilation configurations, and sampling locations used for the HTA contaminant studies: the basic cubical CS Model A; the vertical-noncubical CS Models E2a and E2b, three-times higher and greater volume than CS Model A; and the double-size cubical CS Model Ba, geometrically similar to CS Model A and having eight-times greater volume. Lower case letters were used to designate the specific test configurations for each model.

The test configurations for the HTA studies were selected to provide several comparisons of CS ventilation characteristics.

- o CS Models Aa vs. Ab vs. Ac -- ventilation flow rate variation for the basic cubical model, with flow rate measured in terms of air changes per hour (ACH).
- o CS Models Aa vs. Ba -- doubling all CS model, ventilation, and sampling dimensions (i.e., maintaining geometric similarity) and using the same nondimensional ventilation volume flow rate (ACH) for two cubical models of different size.
- o CS Models Aa vs. E2a -- expanding the cubical model to a vertical-noncubical shape, with the ventilation inlet/outlet (I/O) and sampling elevations moving proportionately to maintain the same nondimensional heights (%H), and maintaining the same nondimensional flow rates (ACH).
- o CS Models Ab vs. E2b -- adding cubical volumes on top of the basic cube to form a vertical-noncubical shape, keeping the dimensional flow rate (cfm) and the dimensional I/O and sampling elevations (inches) the same as for the basic cube.

Figures 4, 5, and 6 are photographs of the experimental facilities. Figure 4 shows a test setup for O_2 recovery from deficiency caused by N_2 for several noncubical CS models. Figure 5 shows the facility configuration for O_2 deficiency caused by HTA contaminants in cubical and noncubical CS models. Figure 6 is a picture of the basic cubical CS Model A and other equipment used for the reduction of simulated (using IBE) toxic contaminant concentrations for comparison to recovery from O_2 deficiency caused by N_2.

A total of 326 experimental cases were tested. These may be summarized as follows:

- o O_2 Recovery for a Cubical CS Model[15]
  - O_2 deficiency caused by N_2
  - 2 ventilation modes (exhaust and supply)
  - 7 volume flow rates (6, 12, 20, 30, 40, 50, 60 ACH)
  - 7 inlet/outlet elevations (15, 25, 40, 50, 60, 80, 100 %H)
  - 98 test cases (= 2 x 7 x 7)
- o O_2 Recovery for Noncubical CS Models[16]
  - O_2 deficiency caused by N_2
  - 2 ventilation modes (exhaust and supply)
  - 3 volume flow rates (20, 40, 60 ACH)
  - 3 inlet/outlet elevations (25, 50, 75 %H)
  - 6 CS models (B, C, D1, D2, E1, E2)
  - 108 test cases (= 2 x 3 x 3 x 6)
- o O_2 Recovery for Heavier-than-Air Contaminants[17]
  - 2 ventilation modes (exhaust and supply)
  - 2 inlet/outlet elevations (25 and 75 %H)
  - 4 contaminants causing O_2 deficiency (N_2, CO_2, HC22, SF_6)
  - 6 CS model/ventilation configurations (Aa, Ab, Ac, E2a, E2b, Ba)
  - 1 flow rate for each test configuration
  - 96 test cases (= 2 x 2 x 4 x 6 x 1)
- o Reduction of Simulated Toxic Concentrations[18]
  - Isobutylene (IBE) to simulate toxic contaminants
  - 2 ventilation modes (exhaust and supply)
  - 4 volume flow rates (10, 20, 40, 60 ACH)
  - 3 inlet/outlet elevations (25, 50, 75 %H)
  - All testing with CS Model A
  - 24 test cases (= 2 x 4 x 3)

Experimental Results

Ventilation performance for O_2 recovery was characterized in two ways: 1) oxygen concentration (%O_2) as a function of ventilation time; and 2) delta T, the time to recover from 10 %O_2 to 20.9 %O_2. Ambient oxygen level measurements varied marginally from a nominal value of 21 %O_2. This established an asymptote for normalization of the experimental data. The nominal value of 20.9 %O_2 was designated to represent effectively complete (99%) oxygen recovery, with a tolerance of 0.1 %O_2.

Figure 7 compares oxygen recovery as a function of ventilation time at the four sampling locations for the exhaust and supply ventilation modes. Comparisons are shown for the specific test parameters of 20 ACH and 40 %H inlet/outlet (I/O) elevation.

Figures 8 and 9 are three-dimensional plots of experimental data to illustrate the effects of three important design parameters: ventilation volume flow rate (ACH), I/O elevation (%H), and delta T (minutes) O_2 recovery time (10 to 20.9 $\%O_2$). These figures show characteristics for exhaust and supply modes at Location 2 (the midplane of the CS model) and at Location 1 (directly below the ventilation I/O) for the forty-nine (= 7 x 7) inlet/outlet (%H) and flow rate (ACH) combinations which were tested for each mode and location.

Figures 10 and 11 present comparisons of O_2 recovery characteristics for N_2 testing of noncubical CS models. Delta T, the times for essentially complete recovery (10 to 20.9 $\%O_2$) are shown. Comparisons are made for low and high flow rates (20 ACH and 60 ACH) at a low I/O elevation (25 %H). The low I/O elevation was selected because it is representative of many actual CS situations. Figure 10 shows O_2 recovery time for sideways CS model expansion by the progression of CS Models A, D1, and E1. Figure 11 compares O_2 recovery times for depthwise expansion in the progression of CS Models A, D2, and E2.

Figures 12 and 13 present oxygen recovery characteristics ($\%O_2$ vs. time) of HTA contaminants for the basic cubical CS Model Aa at a flow rate of 20 ACH. Figure 12 compares results for the lightest (N_2, SG = 0.98) and heaviest (SF_6, SG = 5.05) gases at three sampling elevations (10, 25, and 40 %H) for exhaust and supply ventilation with high (75 %H) I/O elevation. Figure 13 shows O_2 recovery for the same CS Model Aa at 20 ACH, with high (75 %H) and low (25 %H) I/O elevations for all contaminants (N_2, CO_2, HC22, and SF_6) at the lowest (10 %H) sampling elevation.

Figure 14 illustrates effects of changing ventilation volume flow rate on ventilation time, delta T, for oxygen recovery from 10 to 20.9 $\%O_2$, as calculated from empirical oxygen recovery time constants (discussed subsequently). These are data for the basic cubical shape (CS Models Aa, Ab, Ac) for all contaminants under exhaust and supply ventilation with low (25 %H) I/O elevation. Delta T was calculated from empirical data in order for the HTA contaminant data to be consistent with the N_2 data. Initial O_2 levels for nitrogen were nominally 10 $\%O_2$ throughout the CS model. But for HTA contaminants, the initial O_2 concentration varied above and below 10 $\%O_2$, with some very low O_2 concentrations initially near the bottoms of the CS models. It should be kept in mind that complete O_2 recovery often required more time than delta T, sometimes considerably

more, for HTA contaminants having very low initial O_2 levels just to reach (let alone recover from) 10 $\%O_2$.

Figure 15 provides a general comparison of the two cubical models of different size (CS Models Aa and Ba) which were geometrically similar and were ventilated at the same nondimensional volume flow rate of 20 ACH. Data were taken from O_2 recovery curves for thirty-two test cases for these two models. The purpose of this comparison was to evaluate whether findings for small-scale laboratory models could be applied reasonably to larger models, perhaps ultimately to actual confined spaces.

Figure 16 shows IBE (simulated toxic contaminant) reduction and oxygen recovery (nitrogen reduction) data for three test cases: I) supply, 20 ACH, 25 %H; II and III) supply and exhaust, 60 ACH, 50 %H -- all at Location 3. The curves for oxygen recovery were calculated using empirical O_2 recovery time constants and the same ventilation times as for the experimental IBE data.

Figure 17 is a plot of the nondimensional concentration parameter (C/C_0) for eight test cases of IBE reduction and oxygen recovery (exhaust and supply, 20 and 60 ACH, 25 and 75 %H). This figure includes all IBE data in the range from C/C_0 = 0.05 to 0.95. O_2 recovery data were obtained by interpolation between the two experimental O_2 data points nearest the time for each IBE data point.

Discussion of Experimental Results

The oxygen recovery curves of Figure 7 data show that rates of O_2 recovery varied with location in the cubical CS Model A, even with O_2 deficiency caused by N_2, a neutrally-buoyant contaminant. Oxygen recovery was effectively complete at some locations several minutes earlier than at other locations.

The exhaust and supply cases in Figure 7 demonstrated exponential O_2 recovery for all sampling locations, with oxygen concentration increasing rapidly initially, followed by a gradual increase to ambient (21 $\%O_2$). Oxygen recovery at Location 1 for supply ventilation was significantly different from the other locations, increasing very rapidly from the start-up of supply ventilation. This was because Location 1 was aligned with (directly below) the ventilation outlet. Location 4 showed the slowest recovery for both ventilation modes, indicating less effective air mixing (dilution) at this more-distant location. Locations 2 and 3 demonstrated nearly the same oxygen recoveries. Oxygen recovery, overall, was faster for supply ventilation compared to exhaust ventilation.

Figure 8 suggests several design-oriented observations for O_2 recovery caused by N_2 in a cubical CS model. Delta T was significantly greater for exhaust ventilation than it was for supply. Delta T for supply ventilation was not adversely affected (increased significantly) as a function of outlet elevation, except for low flow rates (e.g., especially at 6 ACH). Exhaust and supply modes had comparable recovery times (e.g., less than 10 minutes) in the exhaust "basin" (i.e., less than 60 %H and more than 30 ACH) and in the supply "valley" (i.e., flow rates above 20 ACH). Increasing exhaust flow rate beyond a limit (e.g., 30 ACH for inlets below 80 %H) and supply flow rate beyond a limit (e.g., 20 ACH) resulted in marginal reductions in delta T.

Figure 9 indicates that exhaust ventilation effectiveness, measured as O_2 recovery time (delta T) at Location 1, was not significantly different from Location 2, as a function of either flow rate (ACH) or inlet elevation (%H). However, supply ventilation effectiveness for Location 1 was significantly different and emphasizes the importance of directing ventilation outlets towards work locations inside confined spaces. Delta T for supply ventilation at a Location 1 (aligned with the outlet) was significantly less than for other locations (e.g., Location 2) even at low flow rates. Oxygen recovery for low supply outlet elevations (15 to 25 %H) was very rapid (delta T less than 1.0 min) regardless of flow rate (6 to 60 ACH) at Location 1.

Figure 10 shows changes in oxygen recovery time for sideways CS model expansion (CS Models A, D1, and E1). Delta T increased progressively in the A-D1-E1 progressive sideways expansion. This characteristic was apparent for both exhaust and supply ventilation, with recovery times for supply being less than for exhaust. Location 4, most distant from the I/O opening, was generally slowest to recover for low flow rates (20 ACH), with less variation for the different locations at high flow rates (60 ACH). Location 1, closest to the I/O opening, was significantly different from the other locations only for CS Model A, which was the only one of these CS models to have Location 1 in aligned with the ventilation supply outlet.

Figure 11 compares oxygen recovery times for depthwise expansion in the progression A-D2-E2. These recovery times were generally less than for sideways expansion (Figure 10). Depthwise expansion indicated progressive increases in recovery time, but the effect was less pronounced than for sideways expansion. Location 4 experienced slower recovery for 20 ACH but not for 60 ACH, suggesting that the higher flow rate and velocities caused more complete mixing. Location 1 indicated consistent rapid recovery for supply ventilation for all three of these CS models because the location was in alignment with the ventilation supply outlet.

Mechanical ventilation, in all of the test cases, caused substantially more rapid air mixing, contaminant dilution, and O_2 recovery than could have occurred without it. Figures 12 through 15 show that O_2 recovery from HTA contaminant stratification occurred within periods of time ranging from minutes, with effective ventilation design, to hours for heavy contaminants with poor ventilation design. Preliminary testing indicated that O_2 recovery by diffusion alone required much longer than by mechanical ventilation -- roughly 24-36 hours for the basic cubical CS Model A containing SF_6 causing O_2 deficiency.

Contaminant density had significant effects on ventilation effectiveness. Figures 12 through 14 show that ventilation time generally increased with increasing contaminant density. This effect was most pronounced for the lowest (10 %H) elevation in the CS models, as shown in Figure 12. Differences between contaminants were least evident for effective air mixing, such as caused by low (25 %H) outlet supply ventilation in Figures 13 and 14.

Supply ventilation was generally more effective than was exhaust ventilation. Figures 12 through 14 show supply ventilation causing oxygen recovery in less time than for exhaust under otherwise identical conditions for the CS models. This advantage tended to improve with increasing contaminant density, was greatest at low elevations, and was not affected significantly by CS shape variations. The magnitudes of the differences between supply and exhaust ventilation can be dramatic, e.g., from several minutes for complete O_2 recovery under supply ventilation to an hour or more for HTA contaminants under exhaust ventilation. The reason for more rapid contaminant dilution under supply ventilation is the increased dynamic mixing caused by the airflow jet discharged from the ventilation outlet.

Inlet/outlet (I/O) elevation had significant effects on CS model ventilation effectiveness. Figures 13 and 14 show ventilation time to be significantly less for low (25 %H) I/O elevations compared to higher (75 %H) elevations. This advantage of low I/O over high I/O was most pronounced for high contaminant densities and low CS model elevations (Figure 12).

Ventilation volume flow rate can have significant effects on ventilation time for oxygen recovery. Figure 14 shows ventilation time, delta T, dropping substantially for increasing volume flow rate (ACH) for both supply and exhaust ventilation. This increase was not in proportion to the changes in flow rate. A three-times change from 20 to 60 ACH reduced ventilation time for HTA contaminants by less than 50 percent for exhaust ventilation and by variable amounts with different contaminants for supply ventilation at the lowest (10 %H) sampling elevation, with different characteristics at higher elevations. Reductions in

ventilation time were observed over the full range (20-120 ACH) tested for exhaust ventilation, but there was little improvement above 60 ACH for supply ventilation for the cubical CS Model A.

Geometric similarity is necessary and sufficient for two CS models of different size to experience similar ventilation performance. Similarity must apply for both the CS configuration and the ventilation design. Figure 15 shows that geometric similarity was sufficient for the two cubical CS models (Aa and Ba) of this study to exhibit nearly the same oxygen recovery. It should also be noted that geometric similarity did not exist for CS Model B because the top opening and ventilation pipe sizes and locations were not modified to achieve geometric similarity, as was done for CS Model Ba.

Empirical results from this study are limited to the CS model and ventilation design parameters which were tested. Geometric similarity may make it possible to extend application of the data to larger CS situations, as encountered in the field. However, it is also likely that many field situations will not conform closely enough to the test cases to allow highly accurate predictions of ventilation time.

This study provides some, but limited, consideration of ventilation effects for CS shape variation. Findings for N_2 indicated that "sideways" expansion (CS Models D1, E1) from the basic cubical CS Model A caused some increase in ventilation time for O_2 recovery. "Depthwise" expansion for N_2 (CS Models D2, E2) showed lesser increases in O_2 recovery time than did sideways expansion. However, depthwise expansion (CS Models E2a, E2b) had much more significant effects for HTA contaminants.

Findings for the "expanded" vertical-noncubical CS Model E2a indicated a significant advantage in reducing ventilation time when using low I/O elevation for HTA contaminants. Findings for the "add-on" vertical-noncubical CS Model E2b also demonstrated the importance of providing ventilation near the bottom of a CS containing HTA contaminants. Ventilation characteristics for the basic cube and the "add-on" vertical noncube were quite similar, suggesting that ventilation design for the cubical bottom of a vertical noncube CS may be predicted reasonably well using cubical CS model data, with relatively little shape (depth) effect.

Data in Figures 12 through 14 show that N_2 was not a good predictor of O_2 recovery for HTA contaminant effects. Nitrogen was the only contaminant used in the primary studies of the basic cubical and noncubical CS models. Although not useful for HTA contaminants, findings for nitrogen may be useful for predicting CS dilution ventilation to control toxic contaminants in low concentrations, for which the contaminant mixture

density is nearly the same as that of air and of oxygen-deficient air containing neutrally-buoyant N_2. This is why the N_2 results were compared to results for IBE-simulated toxic concentrations.

Nondimensional parameters were selected for the study of simulated toxic (IBE) concentrations (e.g., Figures 16 and 17) to facilitate broader application in describing and comparing ventilation characteristics. The concentration of IBE was expressed nondimensionally as a fraction (C/C_0) of the initial concentration. The change in C/C_0 is shown as a function of time (minutes) and as a function of the total CS model ventilation air volume CSV (CSV = ACH multiplied by ventilation time in hours).

The concept of total "air change" volume is sometimes applied for dilution ventilation, including confined spaces. The sizes of confined spaces vary greatly, from only slightly larger than the size of a man to many thousands (or even millions) of cubic feet. The capacities (flow rates) of ventilation equipment also vary greatly. Answers to questions on how long to ventilate a CS prior to entry are dependent upon CS size and ventilation flow rate, and can be described in terms of a total number of "air change" volumes.

However, it is important to understand that an "air change" is strictly a calculated parameter and that it is something of a misnomer. It does not mean complete, discrete displacement of contaminated air with fresh replacement air. Contaminant dilution by ventilation is a continuous process which involves the mixing of contaminated air and fresh air. It might be appropriate to describe dilution ventilation in terms of total air volume, e.g., in units of CS volume (CSV), but the inherent limitations of "air changes" must also be considered.

In Figure 16, two CS Model A test cases (I and II) indicated very similar ventilation characteristics, shown by close agreement between the IBE reduction and the O_2 recovery (N_2 reduction) curves. Another case (III), however, demonstrated that IBE reduction and oxygen recovery characteristics can also be significantly different.

The data in Figure 17 generally cluster around the line of agreement (i.e., a slope of 1.0). The points are more diffuse for higher contaminant concentrations (higher C/C_0). Regressional analyses of these data yielded an overall slope of 1.10, with a 95% confidence interval ranging from 0.99 to 1.22. Regressions for the specific locations (1, 2, 3, and 4), flow rates (20 & 60 ACH), and I/O elevations (25 & 75 %H) provided similar results -- slopes ranged between 0.96 and 1.29, with all 95% confidence intervals containing 1.0.

Figure 17 indicates that ventilation characteristics varied, but not greatly even for these greatly different contaminants and concentrations. The largest differences between simulated toxic contaminant (IBE) reduction and O_2 recovery were observed in the early stages of dilution. The tendency for regression slopes to be greater than 1.0 suggests that oxygen recovery was slightly faster than simulated toxic contaminant (IBE) reduction.

Findings from the IBE testing indicate that general ventilation guidelines observed for specific contaminant conditions may apply across a relatively broad range of conditions. For example, both the IBE reduction and O_2 recovery data showed that supply ventilation was consistently more effective than was exhaust. Location 1 was very different from Locations 2, 3, and 4, showing much more rapid contaminant reduction for supply ventilation for locations in alignment with the supply outlet. Results also suggest that highly specific characteristics and design data (e.g., the empirical database from this study) may not apply with great accuracy for significantly different contaminant conditions.

Discussion of Empirical Results

The experimental studies indicated that oxygen recovery occurs in an exponential manner. It does so at significantly different rates for different CS and ventilation configurations and locations. This characteristic can be represented by a simple mathematical model of oxygen concentration ($\%O_2$) as a function of time (t, minutes).

$$\%O_2 = 21 - (21-B)e^{-Ct}$$

In this model, the coefficients (21-B) and C represent the initial oxygen concentration (in $\%O_2$) and an oxygen recovery time constant, respectively. The time constant (C) describes the rate of oxygen recovery from an initial deficiency. This parameter can be used to calculate the ventilation time required for the O_2 level to change from an initial value to a selected final value.

$$\text{Ventilation time (min) for oxygen recovery} = \frac{\ln[(21 - \%O_2 \text{ initial})/(21 - \%O_2 \text{ final})]}{C}$$

The exponential model was used for regression of the experimental O_2 recovery data. The regressions produced an empirical database which describes the experimental test results. The principal empirical parameter, the O_2 recovery time constant (C), is given for each experimental O_2 recovery test case. The regression values of C are tabulated

separately for the exhaust and supply ventilation modes, and for specific CS model parameters, volume flow rates (ACH), I/O elevations (%H), contaminant substances (N_2, CO_2, HC22, SF_6), and CS model locations (1, 2, 3, and 4). The regressions were performed on a personal computer using commercial statistical software (SYSTAT).

Tables I through VI present the regression values of the O_2 recovery time constant (C) for exhaust ventilation (Tables I, III, and V) and supply ventilation (Tables II, IV, and VI). These data are from the three primary O_2 deficiency studies: N_2 testing of cubical CS Model A (Tables I and II), [15] N_2 testing of noncubical CS models (Tables III and IV), [16] and HTA contaminant testing of cubical and noncubical CS models (Tables V and VI). [17]

Most of the values of C for the O_2 recovery (from N_2-caused deficiency) test cases (Tables I - IV) ranged from roughly C = 0.2 (e.g., low flow rate -- 20 ACH, high I/O -- 75 %H) to C = 1.0 (e.g., higher flow rate -- 60 ACH). These C values can be used to calculate ventilation time for oxygen recovery situations of interest. Two examples would be: 1) 90 percent recovery (e.g., from 10 to 20 $\%O_2$), and 2) 99 percent recovery (e.g., from 10 to 20.9 $\%O_2$). Ventilation times calculate to be: 2.4 minutes for 90 percent recovery with C = 1.0, 12.0 minutes for 90 percent recovery with C = 0.2, 4.7 minutes for 99 percent recovery with C = 1.0, and 23.5 minutes for 99 percent recovery with C = 0.2. These data suggest that mechanical ventilation can eliminate oxygen deficiency inside a CS within a relatively brief period of time for a variety of situations.

The C values for HTA contaminants (Tables V and VI) ranged significantly lower, down to C = 0.01 for low CS elevations (e.g., 10 and 25 %H), heavy contaminants (e.g., SF_6), and exhaust ventilation with a high (75 %H) inlet. C values for HTA test cases were generally less than 1.0 for flow rates of 60 ACH and lower. Some data for very high supply ventilation flow rates (e.g., 120 ACH) indicated C values as high as C = 1.5 for lighter contaminants (e.g., N_2 and CO_2) causing O_2 deficiency. The HTA database encompasses a roughly 100-fold range of C data, which corresponds to a 100-fold range of ventilation time O_2 recovery. For practical applications, C = 1.0 represents very rapid recovery (e.g., within a few minutes). There is relatively little benefit, for design purposes, in using C values greater than 1.0.

Some of the regression values of C in Table IV are significantly greater than 1.0. These data are for CS Models A, D2, and E2 (depthwise expansion) for O_2 deficiency caused by N_2 at Location 1 under supply ventilation with a low (25 %H) outlet elevation. These specific C values are the result of regression. For design purposes, these data simply

represent very rapid O_2 recovery. As mentioned previously, there is little practical point in using C values greater than 1.0 for estimating ventilation time.

The regressions were very good approximations of the experimental data. For the entire O_2 recovery time constant (C) database (approx. 300 test cases, 4 locations each case), the coefficient of regression (R^2) averaged roughly 92%. Many of the cases for N_2 had R^2 near 99%. Standard errors (SE) for all data were less than 5%, with SE typically less than 1% for O_2 deficiency caused by N_2. The high R^2 and low SE values support a high level of confidence that the empirical data accurately represent the experimental data.

Extension of the data from this study to significantly different CS configurations would have uncertain effects. If other CS configurations have a larger opening or more than one opening, the ventilation time probably would be less (higher C values). A fully open-top cubical CS Model A, for example, was found to be unable to sustain oxygen deficiency caused by nitrogen, even without mechanical ventilation.[15] Different locations of the top opening could alter ventilation effectiveness. For example, moving the CS opening closer to the center of the space would be expected to improve ventilation effectiveness, increasing C values and decreasing ventilation times. The less effective "corner" location was selected for these studies as a means of providing more conservative results. The presence of internal surfaces and structures could also greatly affect airflow patterns, ventilation effectiveness, and necessary ventilation times inside confined spaces. There are, in short, many important design parameters which have not been tested in these studies.

The empirical database for the O_2 recovery testing using N_2 may have broader application than for O_2 recovery alone. The experimental studies for IBE (simulating toxic concentrations) suggest that general characteristics for O_2 deficiency caused by a neutrally-buoyant contaminant (e.g., N_2) may also apply reasonably well for many situations involving much lower (e.g. potentially toxic) contaminant concentrations. It must also be noted that empirical data for N_2 was not representative of O_2 recovery characteristics from O_2 deficiency caused by significantly heavier-than-air contaminants (e.g., HC22 and SF_6).

Multicellular Ventilation Modeling

The type of ventilation most often used for CS entries is dilution ventilation. Dilution ventilation reduces contaminant concentrations by introducing fresh air to, and removing contaminated air from, the work space. The laboratory testing of CS model ventilation in

the studies described previously has been dilution ventilation to cause O_2 recovery and reduction of simulated toxic (IBE) contaminant concentrations.

Conventional models of dilution ventilation[14] have very limited usefulness for predicting ventilation characteristics for CS situations. Conventional models consider the entire work space as a uniform volume (a "single cell"). The conventional models cannot accurately account for variations in contaminant concentrations caused by airflow patterns which change with the geometric configuration of the space and the design of ventilation in the space. The objective of this part of the study was to develop, by means very different from the conventional approach, dilution ventilation models which could do a reasonably good job of predicting contaminant dilution caused by ventilation in a confined space.

A three-dimensional (3-D) space can be divided into a number (N) of subspaces or cells, thereby creating a multicellular model of the space. Contaminant movement inside the space can be represented as a group of N cells which interact across cell boundaries. Multicellular models assume instantaneous uniform mixing of contaminants within each cell. Reactions of contaminants and buoyancy effects were assumed to be negligible in the multicellular models developed in this study.

Multicellular models have been used to predict contaminant concentrations and ventilation effectiveness in room and workplace environments.[21-24] These ventilation models typically involved simple flow patterns and relatively small numbers of cells. Multicellular models also have been developed for predicting contaminant concentrations in lakes and streams.[25,26] Hydraulic models typically involve more cells than are used for room air models because more cells are needed to represent relatively complex space (lake) geometry and water flow patterns.

Contaminants are transported within a 3-D space by mass flow and dispersion. Dispersion occurs as a result of mechanical dispersion (turbulent mixing/convective diffusion) and molecular diffusion (concentration gradient). For this study, dispersion was treated as a general effect, causing and responding to changes in contaminant concentration between cells, in addition to changes caused by mass flow between the cells. More specifically, dispersion was represented by an empirical dispersion coefficient (D) multiplied by the concentration gradients between cells.

Figure 18 illustrates the concept of contaminant dispersion between cells in a multicellular model. For a typical cell (i), the rate of change of concentration can be described by a mass-balance equation.

$$V_i \frac{dC_i}{dt} = W_i + \sum_{j=1}^{N} Q_{ji} C_j - \sum_{j=1}^{N} Q_{ij} C_i - \sum_{j=1}^{N} D_{ij} A_{ij} \frac{C_i - C_j}{L_{ij}}$$

where
- V_i = volume of cell i, in m^3 (ft^3)
- C_i = contaminant concentration in cell i, in percent (%)
- C_j = contaminant concentration in cell j, in percent (%)
- W_i = contaminant generation rate in cell i, in $\%m^3$/sec ($\%ft^3$/sec)
- Q_{ji} = volume flow rate from cell j to cell i, in m^3/sec (ft^3/sec)
- Q_{ij} = volume flow rate from cell i to cell j, in m^3/sec (ft^3/sec)
- D_{ij} = dispersion coefficient between cell i and cell j, in m^2/sec (ft^2/sec)
- A_{ij} = cross-sectional area between cell i and cell j, in m^2 (ft^2)
- L_{ij} = distance between cell i and cell j, in m (ft)
- t = time, in seconds
- N = number of cells

The multicellular models were Nth-order systems of first-order, initial-value problems. In this study, the Euler method was used to solve the mass balance equation for time-dependent situations, and the Gauss-Seidel iterative method was used for steady-state situations. The model programs were written in FORTRAN 77 and were run on an IBM-AT personal computer.

Multicellular models can be solved when mass or volume flow rates and dispersion coefficients between cells are specified for a given 3-D space and cell structure. In this aspect of the study, cell flow rate and dispersion data were estimated by experimental testing and approximations.

The CS model used for this testing was CS Model A, the same as used for the other experimental studies (described previously) except for installation of a perforated-plenum bottom section. The four sampling locations for measuring $\%O_2$ also were different from the other studies in order to allow evaluation for locations of greater significance for the multicellular models. These experimental studies were conducted in two phases: observation of air flow patterns, and measurements of oxygen deficiency.

Air flow patterns were tested for eight (= 2 x 2 x 2) ventilation configurations: two modes of ventilation (exhaust and supply), at two volume flow rates (20 and 60 ACH), for two inlet/outlet elevations (25 and 75 %H). Air flow patterns were visualized using smoke tubes attached to a probe. Velocities were measured using a nondirectional thermal anemometer.

Twenty-four (= 8 x 3) cases were tested experimentally to evaluate the multicellular models. Each of the eight ventilation configurations was tested for three types of contaminant release (N_2 to cause O_2 deficiency): (1) purging -- O_2 recovery from an initial deficiency, (2) steady state -- constant contaminant (N_2) release rate, and (3) variable rate -- intermittent contaminant release. An oxygen-deficient atmosphere was created by releasing nitrogen uniformly through the perforated-plenum bottom of the cubical CS Model A. The procedure for measuring oxygen deficiency was the same as in the other CS model studies.

Purging data were used to obtain estimates of the dispersion coefficients (D) needed to solve the multicellular model. This involved iterations (trial and error) of multicellular model data using different dispersion coefficients to obtain coefficients which fit the experimental data for purging. Experimental data for the steady-state and variable-rate conditions were used to evaluate predictions of the multicellular model using the dispersion coefficients obtained for purging. A single value of D was selected and used for all cells of the multicellular models for the test cases.

Figure 19 shows air flow patterns observed for the eight ventilation test configurations. The patterns illustrate basic characteristics of air movement into, out from, and within the cubical CS Model A. Within local 3-D regions (e.g., cells), the flow can be described to balance (in-flow = out-flow, for each cell). Uniform flow was assumed across each surface between cells in the multicellular model. The data used to estimate flow rates between cells were developed from nondirectional velocity measurements and visual observations of air flow direction (flow patterns) inside the CS model.

The design of multicellular structures for specific applications addresses two objectives: 1) providing adequate detail and accuracy for predicting contaminant dispersion (ventilation effectiveness), and 2) avoiding unnecessary complexity which can limit useful application of the technique. A primary goal in this study was to design a cell structure using the minimum number of cells that could adequately represent the air flow pattern for a specific CS ventilation configuration. The final designs of the multicellular structures developed in this study were based on the experimental air flow patterns and consensus (among the investigators) approximations.

Figure 20 presents top and front views of the four multicellular structures designed for use in this study. The figure shows the exhaust and supply ventilation modes, with high (75 %H) and low (25 %H) inlet/outlet elevations. The locations of the sampling points are also shown. These points were specifically located inside selected cells to provide data for comparison with multicellular model predictions for the same cells.

The top opening in the CS model was the passage for ventilation air flow into and out from the space; it was represented by either one or two cells. The ventilation pipe section was always one cell. The midplane (50 %H) was coincident with cell surfaces in all configurations. Other details and dimensions of cell design varied between configurations. The region around and below the ventilation pipe experienced the most changes in cell design. The main reason for differences in cell structure between exhaust and supply ventilation was the need to represent the supply "jet" effect by adding one or two cylindrical cells below the ventilation pipe. Symmetry was utilized to a large extent, as shown in the top views of Figure 20, by using some L-shaped cells in all of the test configurations.

Preliminary testing was conducted in which oxygen concentration was measured at more than one location in a given cell. This testing verified that oxygen levels were symmetrical about the diagonal plane through the ventilation opening, and that levels were reasonably uniform within a given cell. Results from the other experimental CS model testing also demonstrated symmetry about the diagonal plane.

Boundary Element Velocity Modeling

Multicellular models require data for three-dimensional (3-D) flow characteristics in order to describe contaminant mass flow between cells. This information is typically obtained by measurement and empirical approximation, such as from the air flow testing of this study. These data help to describe contaminant movement within the 3-D space. This relatively tedious and inexact aspect of the multicellular modeling method (Model 1, described previously) was a significant limitation. This part of the multicellular modeling study (Model 2) investigated the premise that computer approximations might provide more flexible, less tedious, and sufficiently accurate estimates of flow between cells.

This portion of the study focused on the development of a 3-D air flow model for the cubical CS Model A. The air flow model was developed using the Boundary Element Method (BEM), also described as the Boundary Integral Equation Method (BIEM). The BEM was first introduced for industrial ventilation applications as a means to model air flow velocities into free-standing local exhaust inlets. [27]

Multicellular models describe contaminant movement by mass flow and dispersion across the surface boundaries between adjacent cells. The dispersion phenomenon is approximated by an empirical coefficient (D) multiplied by the contaminant concentration differences (gradients) and surface areas between adjacent cells. This BEM-multicellular model (Model 2) used the same dispersion coefficient (D) for both exhaust and supply ventilation. The coefficient had the same value as was used in the previous multicellular Model 1 for exhaust ventilation. It was twice the value used previously for supply ventilation. A higher dispersion coefficient was needed for supply ventilation in this aspect of the study because the BEM model could not represent the supply "jet" effect and the enhanced air and contaminant mixing which it caused.

This aspect of the study utilized BEM to estimate the velocities needed to approximate mass flow across cell boundaries. Contaminant mass flow rates between adjacent cells are functions of the contaminant concentration in each cell and the volume flow rates between cells. Volume flow rates can be described by the average velocities across cell boundary surfaces multiplied by the areas of the surfaces. Surface areas are defined by the design of the cell structure. It is necessary to have some way of approximating the magnitude and direction of average flow velocities across cell boundary surfaces.

A major advantage of BEM is its ability to provide velocity data at any location inside the 3-D space of interest. This was particularly useful for this study because it enabled approximation of air flow velocities on specified cell boundary surfaces. BEM-predicted velocities at several locations on each boundary were averaged and used to estimate volume/mass flow between cells.

Detailed discussions of the mathematical procedures which constitute BEM can be found in the literature. [28-30] The procedures used for this study are described elsewhere. [20] Briefly, BEM is a numerical method to approximate the solution of a governing equation for a phenomenon of interest, throughout and on the boundaries of a spatial domain. BEM provides approximations of unspecified boundary conditions for all elements of the domain boundary by using boundary conditions which are known and specified, and by using functions which satisfy the governing equation.

In this study, the phenomenon of interest (air flow) was assumed to be governed by Laplace's Equation which appiies for incompressible, inviscid, and irrotational flow. Boundary conditions for each boundary element were specified for the scalar function (Φ) called velocity potential or for its normal derivative ($\partial\Phi/\partial n$) which is velocity. The following discussion describes BEM as it was developed and applied for this study.

Figure 21 shows top and front views of the cubical CS model configuration. Boundary conditions on velocity and velocity potential are designated. Velocity potential was specified to be zero at the top opening of the CS model. The normal component of velocity was specified to be 100 at the opening of the ventilation pipe (i.e., 100% of the average pipe velocity, V_0) and zero at all solid boundary surfaces (i.e., no flow through the surface). Boundary surface elements were delineated by nodal points (shown as dots, some very small and slightly larger). The two test configurations of low (25 %H) ventilation pipe inlet/outlet (I/O) and high (75 %H) I/O are shown in Figure 21. An enlargement of the top quadrant containing the ventilation opening and pipe is shown. The four multicellular model sampling locations are also shown.

Modeling Results and Discussion

Figure 22 illustrates volume/mass flow rate data between cells as it was approximated and used for the multicellular Model 1 (i.e., using measured and estimated air flow data). This figure shows cell structures and air flow characteristics for exhaust and supply ventilation, with high flow rate (60 ACH) and low inlet (25 %H) and high outlet (75 %H) elevations. Air flow distribution was characterized by the following: mass balance was maintained in each cell; 100 units of flow entered and left the CS model; units of flow between cells were represented as percentages of the total flow (100 units); and circulatory flow within the CS model was estimated relative to the total flow.

The flow rate data used in this part (Model 1) of the multicellular study were based on the observed air flow patterns and measured velocities inside the CS model. There was an undeniable aspect of subjective judgement in describing the flow rates shown in Figure 22, and in corresponding data for other configurations. The data which were used represented the best judgement and consensus of the investigators.

Figure 23 provides comparisons of Model 1 predictions and experimental data for variable rates of contaminant (nitrogen) release for the case of supply ventilation, 20 ACH at 75 %H. The data represent 10.0 Lpm of nitrogen released over 10 minutes, followed by 30 minutes of no N_2 release. Two complete on/off N_2 release cycles are shown.

Multicellular Model 1 provided reasonably good predictions of oxygen concentration variation with time for variable contaminant release. Linear regressions of multicellular Model 1-predicted O_2 levels versus experimental O_2 levels for the data of Figure 23 yielded slopes of 0.994, 1.000, 0.992, and 1.000 for Locations 1,2,3, and 4, respectively,

with R^2 ranging from 75% to 90%, and SE of model estimates ranging from 0.2% to 0.5% (average confidence of 98.5%).

Figure 24 illustrates that BEM can be used to provide velocity data for specific surfaces inside the CS model. Total velocity magnitude is plotted at two elevations (15 and 50 %H) for a low (25 %H) I/O elevation. It is also possible to plot velocity components for specific flow directions. BEM data such as this were obtained and used for the specific cell surfaces of the multicellular CS ventilation Model 2.

The BEM predictions of air flow patterns are the same for exhaust and supply ventilation except that flow directions are reversed. This is a serious limitation of Model 2 because supply air flow patterns are actually quite different from exhaust because of the existence of the supply "jet." The simple governing equation used in this study, Laplace's Equation, cannot describe the factors (principally, viscosity of the air) which cause the jet effect. The BEM model used in this study also cannot predict circulatory flow patterns inside the CS model, which can exist because of viscosity for both supply and exhaust cases. It would be necessary to solve the much more complex Navier-Stokes Equations in order to address air flow viscosity; this is extremely difficult to do, especially in 3-D.

Figure 25 illustrates results of using BEM velocity data to approximate mass flow between cells for specific cases of the multicellular Model 2. Data show a nominal 100 total units of flow apportioned among the cells. These are examples of the data used to describe the mass flow aspect of contaminant dispersion within the CS model. The cell structures for this study were the same for both exhaust and supply ventilation because the BEM model could not describe the supply jet effect, which was approximated in multicellular Model 1.

Figure 26 presents comparisons of data at the four sampling locations as predicted by the multicellular CS model using BEM velocity data (Model 2), by the multicellular model using empirical velocity data (Model 1), and as measured experimentally. Figure 26 presents steady-state O_2 levels for four test cases (exhaust and supply, 20 ACH, I/O at 25 and 75 %H). Steady-state O_2 levels for exhaust ventilation were in closer agreement than were the levels for supply ventilation. Model 1, overall, was in somewhat closer agreement with experimental data than was Model 2. There did not appear to be any trend on the basis of location, except at Location 1 where Model 2 predicted consistently lower O_2 levels than did Model 1. Variations in O_2 levels at Locations 2,3, and 4 were generally within 2 $\%O_2$ -- relatively good for a computational model, but probably an excessive range relative to predicting safe entry into confined spaces. Model 2 was least effective for the case of high (75 %H) outlet supply ventilation.

Data have not been presented for the higher flow rate, 60 ACH, test cases. These results were similar to what has been presented for 20 ACH, except that variations for Model 2 were sometimes greater because the air flow patterns (Figure 19) for both supply and exhaust ventilation were more complex at 60 ACH. The BEM cannot predict differences in air flow patterns caused by different flow rates.

Guidelines and Recommendations

Findings from the experimental studies on oxygen recovery in CS models help to establish guidelines for CS ventilation design which can be summarized as follows:[17]

- o Air movement caused by mechanical ventilation will greatly enhance contaminant dilution inside a CS. Contaminant dilution caused by diffusion and/or natural ventilation is much slower than dilution caused by mechanical ventilation.
- o Heavier-than-air contaminants can stratify inside confined spaces. Rates of contaminant dilution tend to decrease as contaminant density increases, especially near the bottom of a confined space.
- o Supply ventilation is generally more effective than exhaust in reducing the length of time required for contaminant dilution because air mixing is enhanced by the supply jet. Decisions to ventilate by either supply or exhaust should include consideration of other advantages and disadvantages (discussed subsequently).
- o A directed supply jet of fresh air can provide very effective air mixing and dilution, such as rapid oxygen recovery, at locations aligned with the jet. It is highly advisable in many CS ventilation situations to direct fresh air to the breathing zones of workers.
- o Low ventilation I/O elevations (e.g., less than 25 %H) are generally more effective than higher I/O elevations (e.g., above 75 %H). This characteristic can be very pronounced for HTA contaminants, increasing with contaminant density.
- o Ventilation volume flow rate can have significant effects upon ventilation time. Reductions in ventilation time typically are not proportional to increases in volume flow rate. Benefits from exceeding 60 ACH may be minimal for supply ventilation. Flow rates below 20 ACH are not recommended for most CS ventilation situations.
- o If geometric and air flow similarity (i.e., same CS and ventilation geometry and same ACH) are maintained between two confined spaces of different size, then they will probably have similar ventilation characteristics. If geometric similarity is not maintained, then ventilation characteristics may be very different.
- o The shape of a CS can have significant effects upon ventilation characteristics. HTA contaminants may cause substantial differences for characteristics of cubical versus noncubical shapes, in vertical and horizontal orientations. A cubical CS model may

be able to predict ventilation effects in the "cubical bottom" of a vertical noncubical CS.

- o Variations in ventilation effects with CS shape (e.g., cubical versus noncubical) are less pronounced when contaminant density is not significantly different from air, such as for neutrally-buoyant nitrogen and for toxic contaminants in relatively low concentrations.

Findings from these studies certainly do not address all important aspects of ventilation control for confined spaces. Careful consideration should be given to other important engineering and administrative control measures, to advantages and disadvantages of different ventilation alternatives, and to ventilation equipment, testing, and training.[17]

Mechanical ventilation of a confined space does not preclude the importance of strict administrative control measures for safe CS entry. Both engineering and administrative controls are needed unless they can be confirmed to be unnecessary (and this can be very difficult to do). CS entries should be avoided whenever possible. Confined spaces should always be opened as much as possible prior to entry.

Advantages of supply ventilation for a CS can include: rapid and moveable localized dilution directly to worker breathing zones; it can cause more effective air mixing throughout the CS; and it can accomplish mancooling. Disadvantages include: enhanced dispersion/evaporation of dusts/liquids; contaminant discharge from CS openings; contaminant buildup if supply air is not fresh; and potentially hazardous mancooling with cold ambient temperatures.

Advantages of exhaust ventilation include: the tendency to be nondispersive of contaminants; contaminants can be discharged away from CS openings; localized control is possible if inlets are positioned close to localized sources; and lower general air flow velocities can reduce mancooling effects. Disadvantages of exhaust ventilation include: less effective general air mixing and dilution; the possibility of drawing contaminants through breathing zones; and the possibility of high localized contaminant concentrations.

Local exhaust ventilation (LEV) can be used effectively in confined spaces provided the inlets (hoods) can be kept close enough to localized contaminant sources. LEV offers the possibility of air cleaning to remove contaminants. LEV usually will not have sufficient volume flow rate to satisfy needs for dilution ventilation, if contaminants are not captured at the hood(s).

Natural ventilation, typically caused by wind and/or thermal convection, can have significant effects upon contaminant concentrations in confined spaces. Natural ventilation has the advantage of not being subject to mechanical failure. However, it can also change without warning and should be used only with strict administrative controls. Natural ventilation should be utilized to whatever extent it may exist. However, mechanical ventilation should be required whenever seriously toxic contaminants are present.

Equipment limitations can be significant factors in ventilation design for a particular CS entry. Ventilation time is a function of the fan volume flow rate. Planning and designing for CS ventilation should be made well before an entry is needed in order to be certain that proper and functioning equipment will be available. Ventilation equipment can cause problems for egress, visibility, communications, undesired mancooling, and other aspects of CS entry safety.

Testing before and during CS entries should always involve monitoring for atmospheric contaminants, even when effective mechanical ventilation is in place. Testing prior to and during CS entries should also include observations and measurements of ventilation parameters to help evaluate ventilation effectiveness.

Training for CS entries should include setup and operation of all ventilation equipment for all persons involved in routine entries and emergency rescues. Training should address ventilation testing and the calibration and operation of gas/vapor/oxygen monitoring instruments. It should emphasize "hands-on" experience. Training drills at actual confined spaces, possibly with potentially hazardous contaminants present, are highly recommended in addition to classroom instruction. Training should be repeated on a regular basis to assure adequate preparation and conduct for CS entries.

There will be some CS entries for which mechanical ventilation is impossible, such as when air must be excluded from the CS (e.g., vessels containing pyroforic catalysts) or when CS size and geometry prevent effective ventilation (e.g., long, complex utility tunnels). It is advisable to provide ventilation as close as possible to work areas that cannot be ventilated directly. It is necessary in such situations to place special emphasis on administrative controls to offset the loss of safety resulting from poor or nonexistent ventilation.

Conclusions

The relationships between CS ventilation design parameters (e.g., CS shape, contaminant density, ventilation I/O elevation and volume flow rate, and location within the CS) are very complex. Combining these with other relevant parameters (many not yet studied) would result in an empirical database so complicated as to defy almost any efforts to establish a rational, accurate, and comprehensive computer design model based solely on empirical findings. A truly comprehensive design model for confined space ventilation probably must come from an analytical basis. This requires developing user-friendly computer programs to solve difficult mathematical problems.

Multicellular ventilation computer models were investigated in this study in an effort to predict CS ventilation performance. Two multicellular model variations were studied. Model 1 utilized measured and estimated air flow characteristics and Model 2 used BEM to approximate air flow inside the CS. Both versions (Models 1 and 2) gave comparable and reasonably good predictions of O_2 recovery for different CS locations. However, they did not do so well as to predict steady-state O_2 levels with sufficient accuracy to provide a practical basis for confirming safe O_2 levels or adequate ventilation time prior to entry for work inside a CS.

Significant improvements are needed in the multicellular modeling procedures used here for CS ventilation. Better methods and data for dispersion coefficients (D) are needed. BEM, using Laplace's Equation to govern the air flow, could not adequately address situations involving supply ventilation (which would require a much more complex governing equation, i.e., Navier-Stokes). Much of the multicellular modeling technique developed for this study was tedious and limited to the specific cubical CS Model A configuration which was studied. Although reasonably effective in predicting some specific CS ventilation cases, the practical usefulness of the multicellular modelling method is clearly quite limited at this time.

Research should continue towards development of practical guidelines for effective CS ventilation. More field testing is needed. This would enhance working experience and could improve the predictive capability of laboratory experiments, particularly when done in conjunction with scale-model testing. The development of analytical models should be encouraged. Such models could be tested and evaluated against the empirical database obtained in these studies for oxygen deficiency. There are many additional and untested design parameters, such as different CS model shapes (e.g., cylindrical), internal CS surfaces, more than one CS opening, and CS opening size variation, to list a few.

This study has shown that ventilation causes contaminant reduction in a generally similar manner across a broad range of concentrations, from potentially toxic (ppm) to oxygen-deficient (%) levels. Findings indicated that general guidelines learned under specific test conditions may be reasonably applied to some other conditions. Results also suggested that specific empirical data (e.g., C values for oxygen recovery) may have good accuracy for some CS ventilation situations and may have poor accuracy for other contaminant and CS conditions. Empirical test data could be used in conjunction with safety factors to help provide conservative estimates of ventilation time for contaminant reduction.

Poor ventilation is a defining characteristic of most confined spaces. There is great need to improve the awareness of potential CS atmospheric hazards and of ventilation as a primary means of control. More specific information is needed on methods for implementing effective CS ventilation.

Mechanical ventilation, even lacking solid comprehensive quantitative design criteria, should be used for most confined space entries with a potential for hazardous airborne contaminants. Mechanical ventilation does what no administrative control (e.g., entry attendant, written permit, atmospheric testing, or personal protective equipment) can do -- it will directly reduce concentrations of potentially hazardous air contaminants in confined spaces. If it were used more often, there would be fewer accidents, injuries, over-exposures, and deaths during work in confined spaces.

Acknowledgements

Support for this research by the National Institute for Occupational Safety and Health is gratefully acknowledged. The figures and tables for this paper are taken from articles (Refs. 15 through 20) which have been or will be published in *American Industrial Hygiene Association Journal* and in *Applied Occupational and Environmental Hygiene*. Some portions of the text are taken from these articles with little or no revision.

References

1. Garrison, R.P., and D.R. McFee: Confined Spaces -- A Case for Ventilation. Am. Ind. Hyg. Assoc. J. 47:A708-714 (1986).

2. National Institute for Occupational Safety and Health: Search of Fatality and Injury Records for Cases Related to Confined Spaces. NIOSH Pub. No. 10947. San Diego, CA: Safety Sciences. (1978).

3. National Institute for Occupational Safety and Health: Alert-Request for Assistance in Preventing Occupational Fatalities in Confined Spaces. NIOSH Pub. No. 86-101. Cincinnati, OH (1986).

4. Petit, T.A. Confined Spaces: Avoiding the Hazards. Occ. Health and Safety 52:17-45 (1983).

5. Rekus, J.F.: Invisible Confined-Space Hazards Require Comprehensive Entry Program. Occ. Health and Safety 59:8:38-42 (1990).

6. Brief, R.S., L.W. Raymond, W.H. Meyer, and J.D. Yoder: Better Ventilation for Close-Quarter Work Spaces. Air Cond. Heat. & Vent. 58:74-88 (1961).

7. Mignone, A.T., E.C. Beckhusen, K.O. Leary, and M. Gochfield: Temporal Variation in Oxygen and Chemical Concentration in a Confined Workspace: The Wastewater Manhole. App. Occup. Environ. Hyg. 5:428-434 (1990).

8. National Institute for Occupational Safety and Health: Criteria for a Recommended Standard -- Working in Confined Spaces. NIOSH Pub. No. 80-106. Washington, D.C.: Government Printing Office (1979).

9. National Institute for Occupational Safety and Health: Safety and Health in Confined Workplaces for the Construction Industry -- A Training Resource Manual. p. 128. Cincinnati, OH (1985).

10. Occupational Safety and Health Administration: Proposed Standard for Permit Entry Confined Spaces, 54 CFR 24080, Washington, D.C.: Government Printing Office (1989).

11. Garrison, R.P.: Ventilation for Work in Confined Spaces. Testimony on the proposed OSHA Standard for Permit Entry Confined Spaces (54 CFR 24080), delivered at an informal hearing in Chicago, Feb. 2, 1990. Washington, D.C.: U.S. Dept. of Labor/OSHA, Technical Data Center, Docket Office (1990).

12. Garrison, R.P.: Comments and Guidelines on Ventilation for Work in Confined Spaces. Follow-up on Testimony, submitted May 2, 1990. Washington, D.C.: OSHA Technical Data Center (1990).

13. American National Standards Institute: Safety Requirements for Confined Spaces. ANS1 Z117.1 - 1989. Des Plaines, IL: Am. Soc. of Safety Engineers (1989).

14. American Conference of Governmental Industrial Hygienists: Industrial Ventilation -- A Manual of Recommended Practice. 20th ed., Cincinnati, OH: ACGIH, Inc. (1989).

15. Garrison, R.P., R. Nabar, and M. Erig: Ventilation to Eliminate Oxygen Deficiency in Confined Spaces -- Part I: A Cubical Model. Appl. Ind. Hyg. 4:1-11 (1989).

16. Garrison, R.P., and M. Erig: Ventilation to Eliminate Oxygen Deficiency in Confined Spaces -- Part II: Noncubical Models. Appl. Ind. Hyg. 4:260-268 (1989).

17. Garrison, R.P., and M. Erig: Ventilation to Eliminate Oxygen Deficiency in Confined Spaces -- Part III: Heavier-than-Air Characteristics. Appl. Occup. Environ. Hyg. 6:131-140 (1990).

18. Garrison, R.P., K. Lee, and C. Park: Contaminant Reduction by Ventilation in a Confined Space Model -- Simulated Toxic Concentrations vs. Oxygen Deficiency. Am. Ind. Hyg. Assoc. J., under peer review (1991).

19. Park, C., and R.P. Garrison: Multicellular Model for Contaminant Dispersion and Ventilation Effectiveness with Application for Oxygen Deficiency in a Confined Space. Am. Ind. Hyg. Assoc. J. 51:70-78 (1990).

20. Park, C., and R.P. Garrison: Boundary Element Method to Approximate Three-Dimensional Velocity Characteristics for a Multicellular Model of Ventilation for a Confined Space. Am. Ind. Hyg. Assoc. J., under peer review (1991).

21. Sinden, F.W.: Multi-Chamber Theory of Air Infiltration. Build. Environ. 13:21-28 (1978).

22. Sandberg, M.: What Is Ventilation Efficiency? Build. Environ. 16:123-135 (1981).

23. Siren, K.E.: A Procedure for Calculating Concentration Histories in Dwellings. Build. Environ. 23:103-114 (1988).

24. Waters, J.R., and M.W. Simons: The Evaluation of Contaminant Concentrations and Airflows in a Multizone Model of a Building. Build. Environ. 22:305-315 (1987).

25. Canale, R.P., and J. Squire: A Model for Total Phosphorus in Saginaw Bay. J. Great Lakes Res. 2:364-373 (1976).

26. Thomann, R.V., and J.A. Mueller: Principles of Surface Water Quality Modeling and Control. pp. 71-76, 206-213. New York: Harper & Row (1987).

27. Flynn, M.R., and C.T. Miller: The Boundary Integral Equation Method (BIEM) for Modeling Local Exhaust Hood Flow Fields. Am. Ind. Hyg. Assoc. J. 50:281-288 (1989).

28. Zienkiewicz, O.C., D.W. Kelly, and P. Bettess: The Coupling of the Finite Element Method and Boundary Solution Procedures. Int. J. Numer. Methods Eng. 11:355-375 (1977).

29. Brebbia, C.A., J.C.F. Telles, and L.C. Wrobel: Boundary Element Techniques. pp. 58-59. Heidelberg: Springer-Verlag Berlin (1984).

30. Ligett, J.A., and P.L.F. Lu: The Boundary Integral Equation Method for Porous Media Flow. pp. 17-18. London: Gorge, Allen & Unwin (1983).

Table I
Regression Values of the Oxygen Recovery Time Constant (C) for Exhaust Ventilation in Cubical CS Model A for Oxygen Deficiency Caused by Nitrogen (Ref. 15)

CS Model Parameters		Oxygen Recovery Time Constant (C)			
		CS Location			
Inlet Elevation (%H)	Volume Flow Rate (ACH)	1	2	3	4
15	6	0.17	0.18	0.17	0.15
	12	0.23	0.23	0.23	0.19
	20	0.27	0.30	0.26	0.26
	30	0.54	0.54	0.54	0.44
	40	0.69	0.63	0.63	0.58
	50	0.80	0.67	0.67	0.70
	60	0.81	0.76	0.72	0.78
25	6	0.17	0.18	0.18	0.15
	12	0.22	0.22	0.23	0.18
	20	0.33	0.34	0.36	0.27
	30	0.44	0.51	0.55	0.43
	40	0.70	0.61	0.61	0.67
	50	0.81	0.71	0.74	0.74
	60	1.03	0.88	0.81	0.92
40	6	0.18	0.19	0.18	0.15
	12	0.24	0.23	0.25	0.20
	20	0.37	0.38	0.38	0.30
	30	0.60	0.56	0.55	0.52
	40	0.69	0.63	0.62	0.64
	50	0.84	0.77	0.76	0.77
	60	0.91	0.76	0.84	0.85
50	6	0.22	0.23	0.23	0.19
	12	0.23	0.24	0.24	0.20
	20	0.35	0.36	0.36	0.30
	30	0.60	0.59	0.58	0.56
	40	0.72	0.66	0.65	0.69
	50	0.88	0.74	0.79	0.85
	60	0.92	0.81	0.81	0.84
60	6	0.14	0.14	0.14	0.12
	12	0.23	0.23	0.24	0.19
	20	0.32	0.34	0.33	0.27
	30	0.55	0.51	0.49	0.52
	40	0.60	0.55	0.60	0.58
	50	0.73	0.66	0.67	0.67
	60	0.88	0.69	0.83	0.80
80	6	0.17	0.17	0.18	0.16
	12	0.18	0.20	0.20	0.17
	20	0.30	0.28	0.27	0.24
	30	0.45	0.40	0.39	0.35
	40	0.51	0.48	0.48	0.48
	50	0.69	0.69	0.65	0.71
	60	0.84	0.73	0.81	0.77
100	6	0.12	0.12	0.12	0.11
	12	0.14	0.15	0.14	0.13
	20	0.16	0.16	0.16	0.15
	30	0.21	0.21	0.22	0.18
	40	0.20	0.20	0.20	0.21
	50	0.23	0.22	0.23	0.23
	60	0.24	0.25	0.24	0.23

Table II
Regression Values of the Oxygen Recovery Time Constant (C) for Supply Ventilation in Cubical CS Model A for Oxygen Deficiency Caused by Nitrogen (Ref. 15)

CS Model Parameters		Oxygen Recovery Time Constant (C)			
		CS Location			
Outlet Elevation (%H)	Volume Flow Rate (ACH)	1	2	3	4
15	6	8.94	0.29	0.29	0.15
	12	10.45	0.50	0.49	0.28
	20	6.72	0.69	0.69	0.38
	30	10.73	0.96	0.98	0.65
	40	6.34	0.86	0.94	0.89
	50	9.71	0.84	0.90	0.82
	60	10.01	0.99	0.97	0.95
25	6	6.30	0.27	0.27	0.11
	12	7.44	0.50	0.48	0.28
	20	10.60	0.76	0.75	0.44
	30	0.32	0.91	0.88	0.63
	40	8.12	0.82	0.87	0.81
	50	4.39	0.86	0.89	0.82
	60	5.56	0.98	1.06	1.01
40	6	0.22	0.10	0.09	0.08
	12	0.77	0.43	0.43	0.23
	20	0.94	0.68	0.66	0.41
	30	0.86	0.76	0.74	0.62
	40	0.84	0.75	0.76	0.73
	50	0.89	0.86	0.86	0.85
	60	1.07	1.01	1.01	1.01
50	6	0.87	0.29	0.29	0.16
	12	0.82	0.49	0.47	0.31
	20	1.14	0.65	0.63	0.42
	30	1.25	0.60	0.63	0.51
	40	1.22	0.70	0.71	0.70
	50	1.79	0.79	0.80	0.80
	60	1.88	0.92	1.01	0.98
60	6	0.61	0.34	0.34	0.21
	12	0.59	0.43	0.43	0.28
	20	1.05	0.59	0.60	0.40
	30	1.05	0.65	0.68	0.57
	40	1.04	0.67	0.73	0.70
	50	1.55	0.77	0.85	0.81
	60	1.71	0.93	0.96	0.97
80	6	0.20	0.16	0.15	0.13
	12	0.30	0.34	0.29	0.23
	20	0.62	0.49	0.52	0.42
	30	0.73	0.59	0.56	0.56
	40	0.64	0.71	0.72	0.73
	50	0.92	0.87	0.80	0.86
	60	0.87	0.92	0.86	0.95
100	6	0.13	0.13	0.12	0.11
	12	0.27	0.26	0.27	0.22
	20	0.45	0.40	0.43	0.40
	30	0.72	0.58	0.57	0.56
	40	0.89	0.71	0.71	0.71
	50	1.01	0.82	0.76	0.81
	60	1.19	0.97	0.86	0.98

Table III.
Regression Values of the Oxygen Recovery Time Constant (C) for Exhaust Ventilation in Cubical and Noncubical CS Models A, B, C, D1, E1, D2, and E2 for Oxygen Deficiency Caused by Nitrogen (Ref. 16)

CS Model Parameters			Oxygen Recovery Time Constant (C)						
			CS Model Configuration						
Inlet Elevation	Volume Flow Rate	Location	Basic Cubical Model	Sideways Expansion (x2)	(x3)	Depthwise Expansion (x2)	(x3)	Multi-directional (2D)	(3D)
(%H)	(ACH)	(1-4)	A	D1	E1	D2	E2	C	B
25	20	1	0.33	0.35	0.31	0.34	0.35	0.29	0.30
		2	0.34	0.34	0.31	0.32	0.32	0.30	0.29
		3	0.36	0.33	0.30	0.33	0.33	0.32	0.28
		4	0.27	0.35	0.24	0.29	0.30	0.25	0.29
	40	1	0.70	0.58	0.49	0.70	0.70	0.48	0.50
		2	0.61	0.53	0.49	0.60	0.69	0.47	0.48
		3	0.61	0.54	0.44	0.60	0.60	0.51	0.48
		4	0.67	0.53	0.42	0.59	0.58	0.48	0.49
	60	1	1.03	0.75	0.56	0.88	0.88	0.61	0.68
		2	0.88	0.73	0.58	0.86	0.86	0.57	0.58
		3	0.81	0.70	0.55	0.80	0.86	0.68	0.60
		4	0.92	0.73	0.54	0.86	0.82	0.62	0.62
50	20	1	0.35	0.31	0.34	0.37	0.35	0.32	0.30
		2	0.36	0.31	0.33	0.34	0.33	0.31	0.30
		3	0.36	0.31	0.27	0.34	0.32	0.34	0.27
		4	0.30	0.30	0.23	0.30	0.30	0.26	0.29
	40	1	0.72	0.57	0.45	0.67	0.64	0.48	0.51
		2	0.66	0.55	0.48	0.60	0.60	0.47	0.50
		3	0.65	0.55	0.40	0.60	0.60	0.49	0.46
		4	0.69	0.56	0.35	0.58	0.55	0.45	0.45
	60	1	0.92	0.81	0.62	0.90	0.91	0.53	0.62
		2	0.81	0.71	0.65	0.83	0.84	0.52	0.59
		3	0.81	0.76	0.55	0.82	0.83	0.58	0.58
		4	0.84	0.76	0.56	0.80	0.80	0.54	0.64
75	20	1	0.18	0.30	0.31	0.36	0.37	0.24	0.26
		2	0.20	0.29	0.30	0.33	0.34	0.24	0.25
		3	0.20	0.29	0.27	0.33	0.34	0.23	0.26
		4	0.17	0.24	0.25	0.32	0.33	0.20	0.25
	40	1	0.30	0.49	0.42	0.64	0.67	0.28	0.32
		2	0.28	0.48	0.41	0.56	0.61	0.29	0.32
		3	0.27	0.47	0.42	0.56	0.61	0.29	0.33
		4	0.24	0.49	0.38	0.50	0.58	0.27	0.34
	60	1	0.51	0.72	0.52	0.89	0.91	0.30	0.44
		2	0.48	0.63	0.54	0.76	0.83	0.32	0.41
		3	0.48	0.64	0.48	0.80	0.80	0.31	0.45
		4	0.48	0.65	0.50	0.79	0.79	0.30	0.45

Table IV
Regression Values of the Oxygen Recovery Time Constant (C) for Supply Ventilation in Cubical and Noncubical CS Models A, B, C, D1, E1, D2, and E2 for Oxygen Deficiency Caused by Nitrogen (Ref. 16)

CS Model Parameters			Oxygen Recovery Time Constant (C)						
			CS Model Configuration						
Outlet Elevation	Volume Flow Rate	Location	Basic Cubical Model	Sideways Expansion (x2)	(x3)	Depthwise Expansion (x2)	(x3)	Multi-directional (2D)	(3D)
(%H)	(ACH)	(1-4)	A	D1	E1	D2	E2	C	B
25	20	1	10.60	0.38	0.30	8.50	7.30	0.30	0.28
		2	0.76	0.42	0.30	0.62	0.51	0.32	0.29
		3	0.75	0.40	0.31	0.62	0.49	0.30	0.28
		4	0.44	0.32	0.28	0.42	0.43	0.27	0.27
	40	1	8.10	0.54	0.48	7.00	6.00	0.52	0.51
		2	0.82	0.49	0.45	0.70	0.57	0.48	0.50
		3	0.87	0.48	0.48	0.78	0.70	0.54	O.51
		4	0.81	0.46	0.45	0.68	0.56	0.51	0.52
	60	1	5.60	0.72	0.71	5.30	5.00	0.77	0.72
		2	0.98	0.71	0.68	0.90	0.83	0.73	0.76
		3	1.06	0.68	0.71	1.00	0.95	0.78	0.77
		4	1.01	0.67	0.71	0.90	0.85	0.74	0.82
50	20	1	1.14	0.36	0.30	0.83	0.51	0.30	0.29
		2	0.65	0.41	0.27	0.51	0.42	0.31	0.30
		3	0.63	0.36	0.29	0.56	0.50	0.29	0.29
		4	0.42	0.30	0.25	0.40	0.43	0.27	0.26
	40	1	1.22	0.54	0.51	1.10	0.83	0.53	0.51
		2	0.70	0.55	0.44	0.66	0.64	0.47	0.53
		3	0.71	0.51	0.46	0.70	0.70	0.50	0.53
		4	0.70	0.50	0.43	0.60	0.71	0.48	0.53
	60	1	1.88	0.77	0.72	1.50	1.16	0.75	0.77
		2	0.92	0.79	0.68	0.92	0.90	0.70	0.79
		3	1.01	0.77	0.70	0.99	1.00	0.71	0.80
		4	0.98	0.76	0.65	0.90	1.00	0.72	0.80
75	20	1	0.62	0.32	0.26	0.53	0.41	0.29	0.34
		2	0.49	0.34	0.24	0.42	0.38	0.30	0.34
		3	0.52	0.32	0.24	0.45	0.38	0.29	0.34
		4	0.42	0.28	0.22	0.40	0.37	0.28	0.34
	40	1	0.64	0.55	0.49	0.90	0.72	0.51	0.61
		2	0.71	0.52	0.41	0.70	0.68	0.48	0.61
		3	0.72	0.50	0.44	0.69	0.68	0.50	0.62
		4	0.73	0.48	0.41	0.69	0.68	0.48	0.63
	60	1	0.87	0.71	0.72	0.92	1.12	0.75	0.90
		2	0.92	0.78	0.65	1.00	1.00	0.71	0.93
		3	0.86	0.76	0.67	1.00	1.10	0.72	0.90
		4	0.95	0.79	0.63	1.00	1.10	0.73	0.90

Table V
Regression Values of the Oxygen Recovery Time Constant (C) for Exhaust Ventilation in Cubical CS Model A for Oxygen Deficiency Caused by Heavier-than-Air Contaminants (Ref. 17)

CS Model Parameters				Oxygen Recovery Time Constant (C) Contaminant (Specific Gravity)			
Config-uration	Inlet Elevation (%H)	Volume Flow Rate (ACH)	Location Elevation (%H)	N_2 (0.98)	CO_2 (1.50)	HC22 (3.00)	SF_6 (5.05)
Aa	25	20	10.0	0.27	0.10	0.07	0.05
			25.0	0.50	0.41	0.41	0.30
			40.0	0.62	0.61	0.61	0.44
			70.0	1.00	1.20	1.23	1.00
	75		10.0	0.32	0.02	0.013	0.012
			25.0	0.30	0.021	0.017	0.016
			40.0	0.32	0.043	0.036	0.035
			70.0	0.32	1.00	0.82	1.30
Ab	25	60	10.0	0.90	0.25	0.13	0.09
			25.0	0.80	1.10	1.00	0.73
			40.0	0.82	1.50	1.30	1.00
			70.0	0.82	2.40	2.20	1.70
	75		10.0	0.70	0.04	0.021	0.010
			25.0	0.61	0.045	0.027	0.011
			40.0	0.67	0.10	0.05	0.021
			70.0	0.67	1.20	0.80	0.50
Ac	25	120	10.0	1.20	0.50	0.20	0.14
			25.0	1.00	1.50	1.70	2.00
			40.0	1.00	2.10	2.30	2.50
			70.0	1.10	2.40	3.00	2.50
	75		10.0	0.95	0.055	0.04	0.014
			25.0	0.88	0.10	0.05	0.015
			40.0	0.80	0.24	0.22	0.04
			70.0	0.85	1.50	0.20	1.40
E2a	25	20	10.0	0.35	0.03	0.026	0.02
			25.0	0.33	1.00	0.60	0.50
			40.0	0.33	1.30	0.80	0.70
			70.0	0.33	1.50	1.40	1.10
	75		10.0	0.32	0.017	0.016	0.012
			25.0	0.32	0.02	0.045	0.035
			40.0	0.31	0.05	0.11	0.10
			70.0	0.33	2.00	2.00	2.40
E2b	8.3	20	3.3	0.90	0.17	0.11	0.09
			8.3	0.80	0.80	1.00	0.79
			13.3	0.80	1.00	1.50	1.00
			23.3	0.80	1.50	2.40	2.30
	25		3.3	0.70	0.022	0.018	0.014
			8.3	0.60	0.029	0.026	0.015
			13.3	0.70	0.06	0.06	0.022
			23.3	0.70	0.08	0.85	0.60

Table VI
Regression Values of the Oxygen Recovery Time Constant (C) for Supply Ventilation in Cubical CS Model A for Oxygen Deficiency Caused by Heavier-than-Air Contaminants (Ref. 17)

CS Model Parameters				Oxygen Recovery Time Constant (C) Contaminant (Specific Gravity)			
Configuration	Outlet Elevation (%H)	Volume Flow Rate (ACH)	Location Elevation (%H)	N_2 (0.98)	CO_2 (1.50)	HC22 (3.00)	SF_6 (5.05)
Aa	25	20	10.0	0.84	0.30	0.16	0.11
			25.0	0.83	0.30	0.30	0.20
			40.0	0.80	0.31	0.30	0.30
			70.0	0.51	0.31	0.30	0.40
	75		10.0	0.41	0.10	0.04	0.027
			25.0	0.38	0.11	0.05	0.032
			40.0	0.41	0.20	0.11	0.087
			70.0	0.40	0.44	0.60	0.50
Ab	25	60	10.0	0.89	0.83	0.81	0.69
			25.0	0.86	0.84	0.81	0.69
			40.0	0.92	0.88	0.82	0.69
			70.0	0.92	0.89	0.81	0.68
	75		10.0	0.92	0.75	0.48	0.20
			25.0	0.88	0.74	0.49	0.30
			40.0	0.94	0.82	0.69	0.53
			70.0	0.92	0.83	0.70	0.60
Ac	25	120	10.0	1.40	1.50	1.20	0.65
			25.0	1.40	1.50	1.30	0.80
			40.0	1.40	1.00	1.30	0.80
			70.0	1.48	1.40	1.20	0.65
	75		10.0	1.50	1.50	0.70	0.60
			25.0	1.60	1.40	0.80	0.65
			40.0	1.55	1.40	0.70	0.70
			70.0	1.60	1.30	0.50	0.70
E2a	25	20	10.0	0.61	0.30	0.28	0.20
			25.0	0.61	0.30	0.37	0.30
			40.0	0.61	0.30	0.37	0.35
			70.0	0.59	0.31	0.37	0.30
	75		10.0	0.41	0.14	0.14	0.07
			25.0	0.42	0.20	0.20	0.12
			40.0	0.42	0.39	0.43	0.30
			70.0	0.42	0.43	0.42	0.25
E2b	8.3	20	3.3	0.90	0.70	1.00	0.68
			8.3	0.86	0.50	0.87	0.69
			13.3	0.92	0.53	0.77	0.69
			23.3	0.92	0.54	0.80	0.60
	25		3.3	0.90	0.45	0.40	0.20
			8.3	0.90	0.42	0.55	0.33
			13.3	0.92	0.44	0.67	0.55
			23.3	0.92	0.43	0.70	0.63

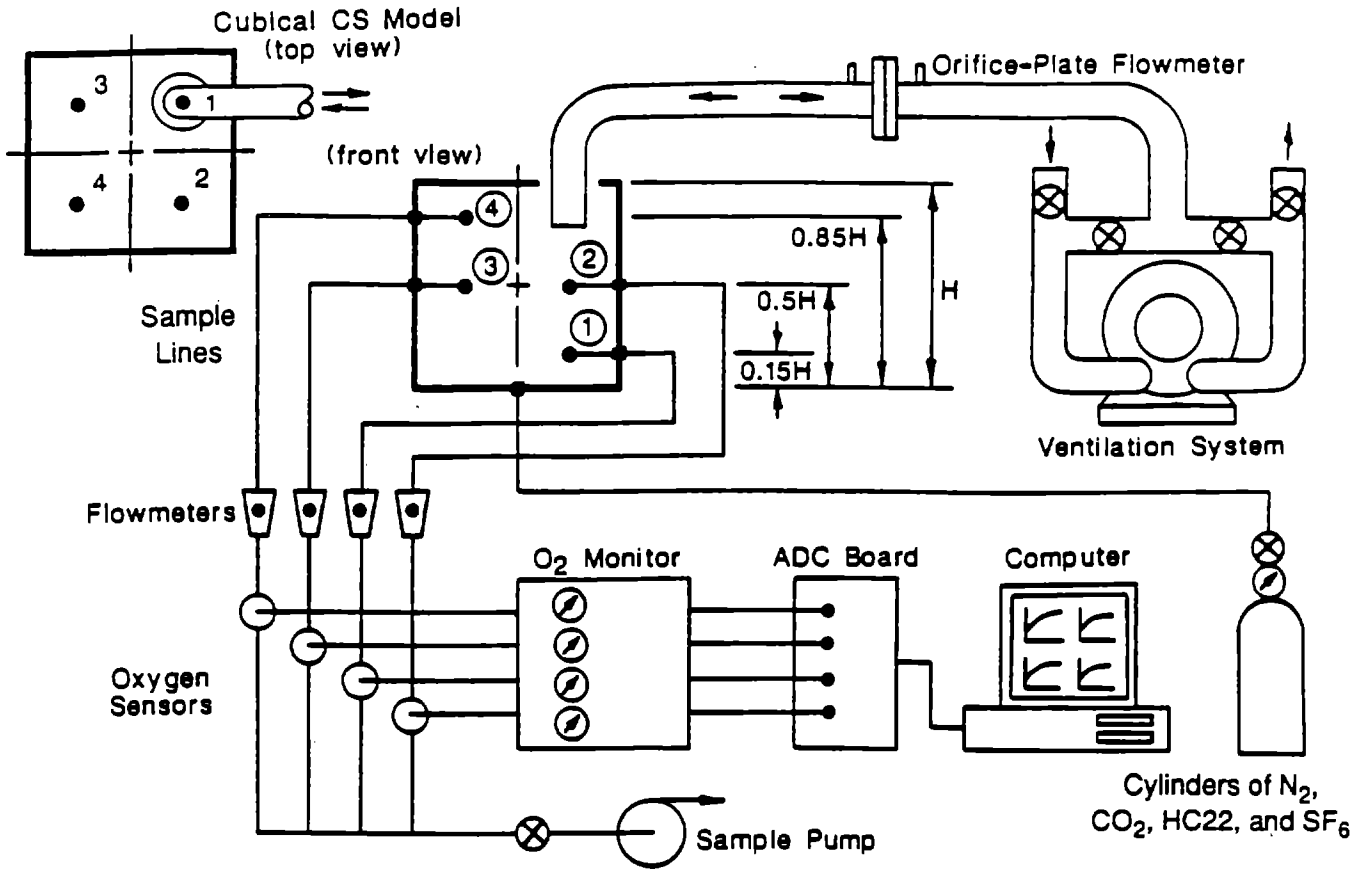

Facility for Oxygen Recovery Testing

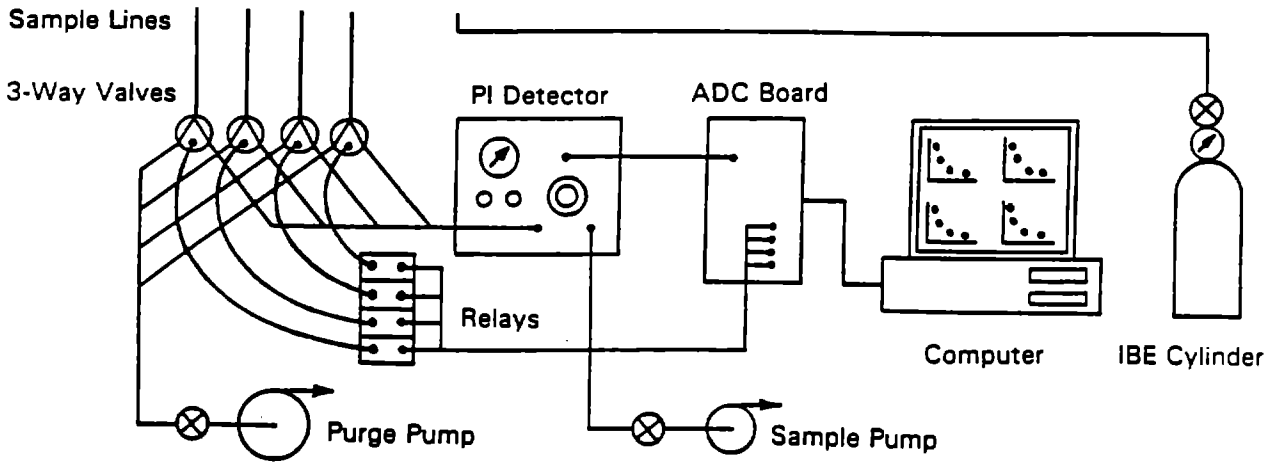

Partial Facility for IBE Testing

Figure 1 – Diagrams of the experimental facility for oxygen recovery testing with different contaminants, and of the sampling and monitoring portion of the facility for testing simulated toxic (IBE) concentrations (Refs. 15 and 18).

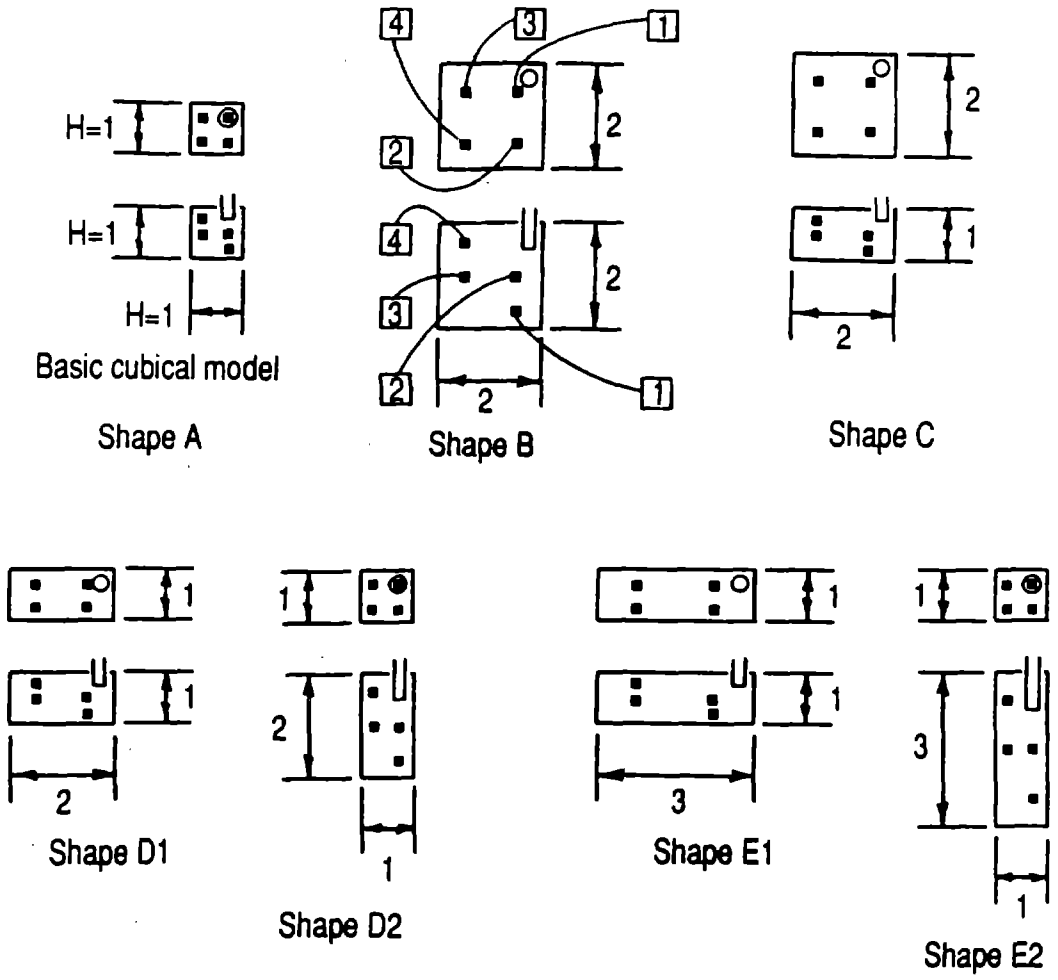

Figure 2 – Cubical and noncubical CS model configurations and sampling locations for oxygen deficiency caused by nitrogen (Ref. 16).

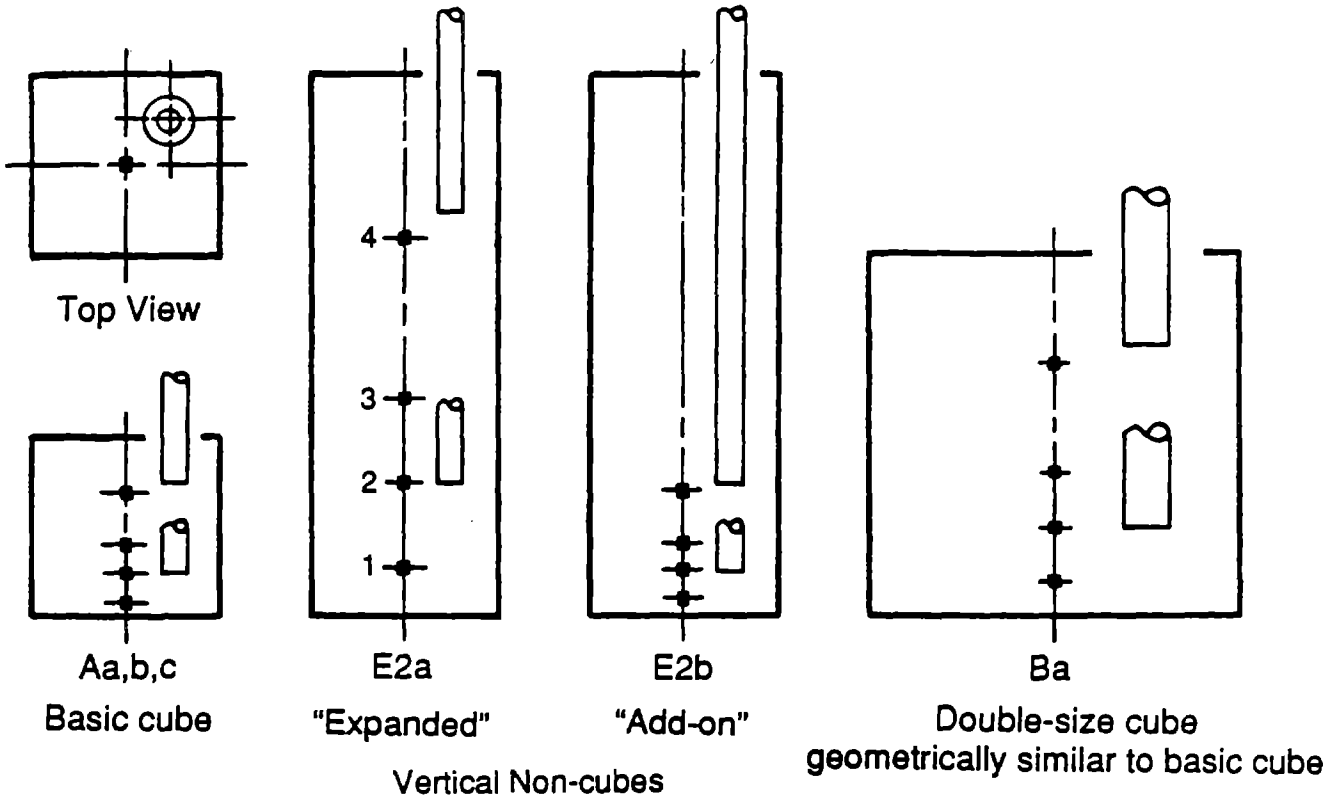

Figure 3 – Cubical and noncubical CS model configurations and sampling locations for oxygen deficiency caused by heavier-than-air contaminants (Ref. 17).

Figure 4 – Experimental test facility for oxygen deficiency caused by N_2 with noncubical CS Models C, D2, and E2 (Ref. 16).

Figure 5 – Experimental test facility for oxygen deficiency caused by N_2, CO_2, HC22, and SF_6 with CS Models A, B, and E2 (Ref. 17).

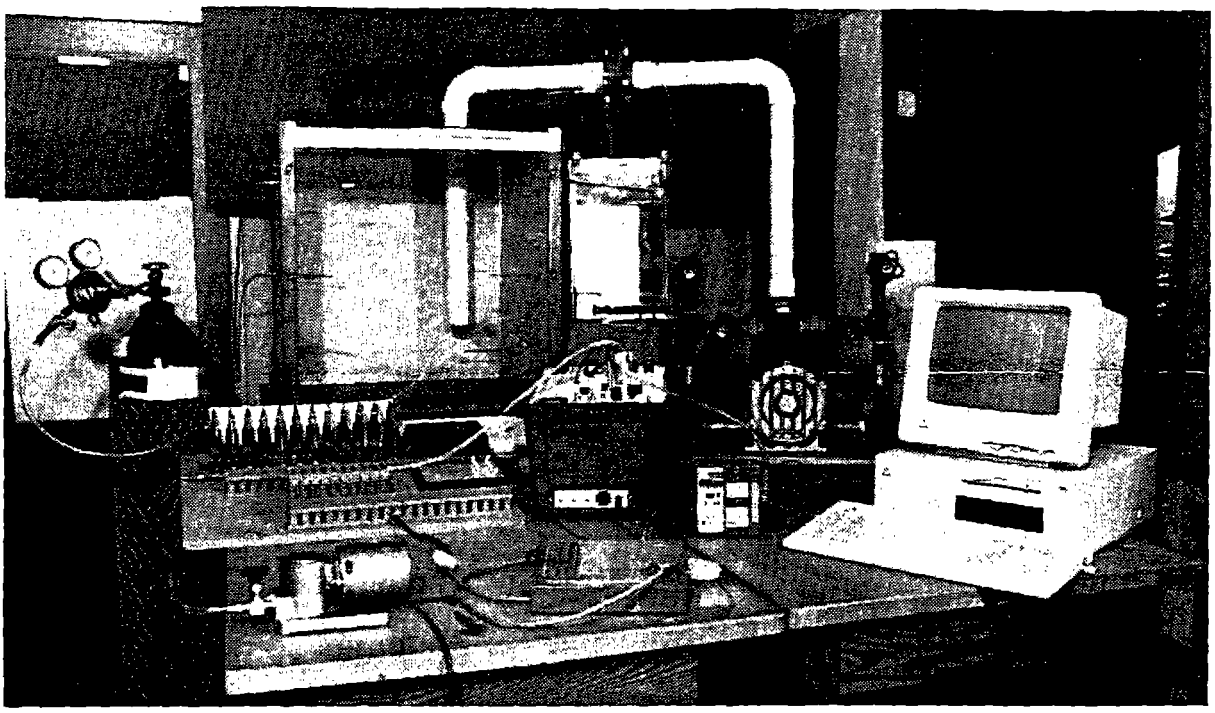

Figure 6 – Experimental test facility for simulated toxic concentrations using IBE with the basic cubical CS Model A (Ref. 18).

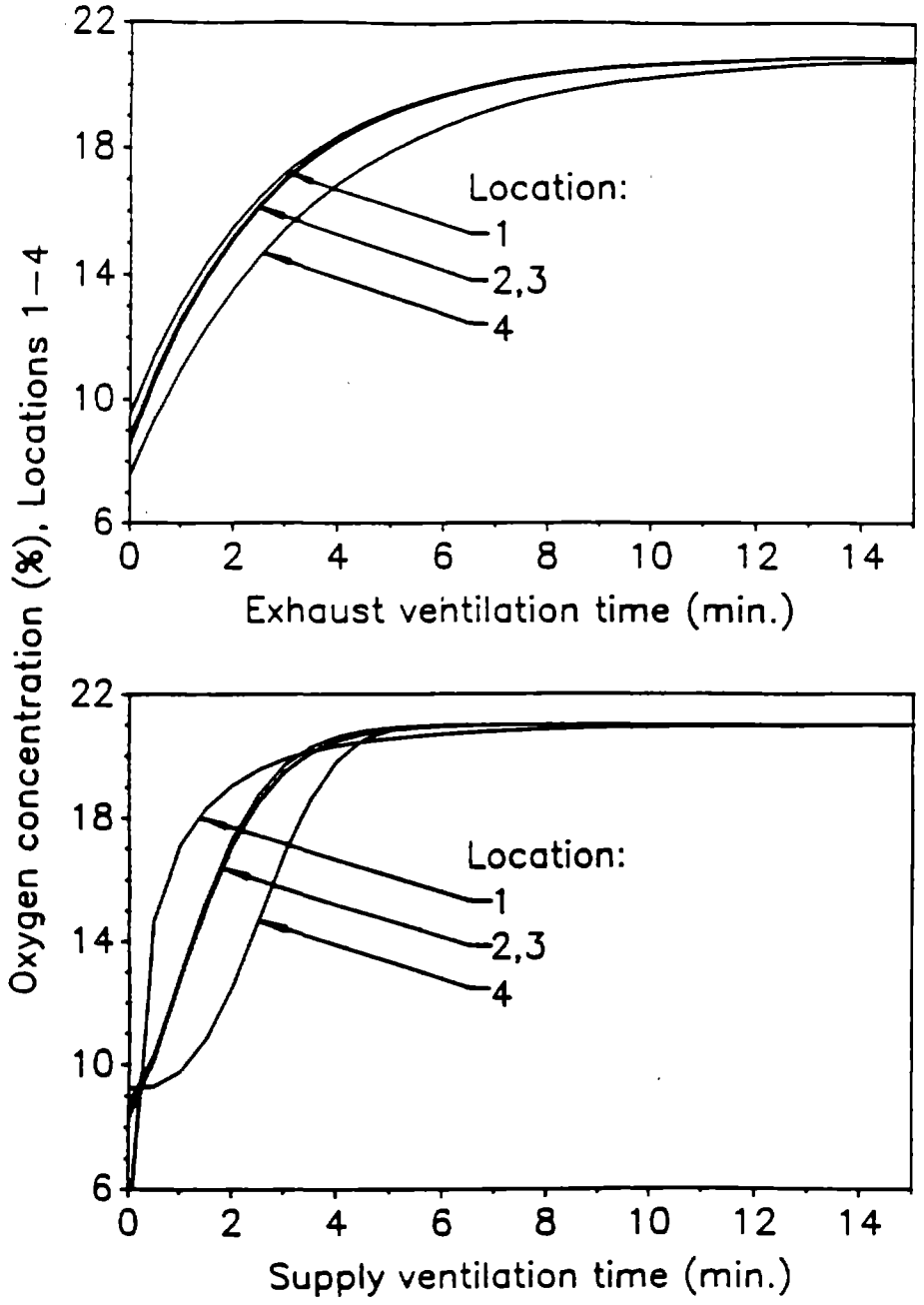

Figure 7 – Oxygen recovery at different sampling locations for exhaust and supply ventilation of the basic cubical CS Model A with O_2 deficiency caused by N_2 (20 ACH, I/O 40 %H, Ref. 15).

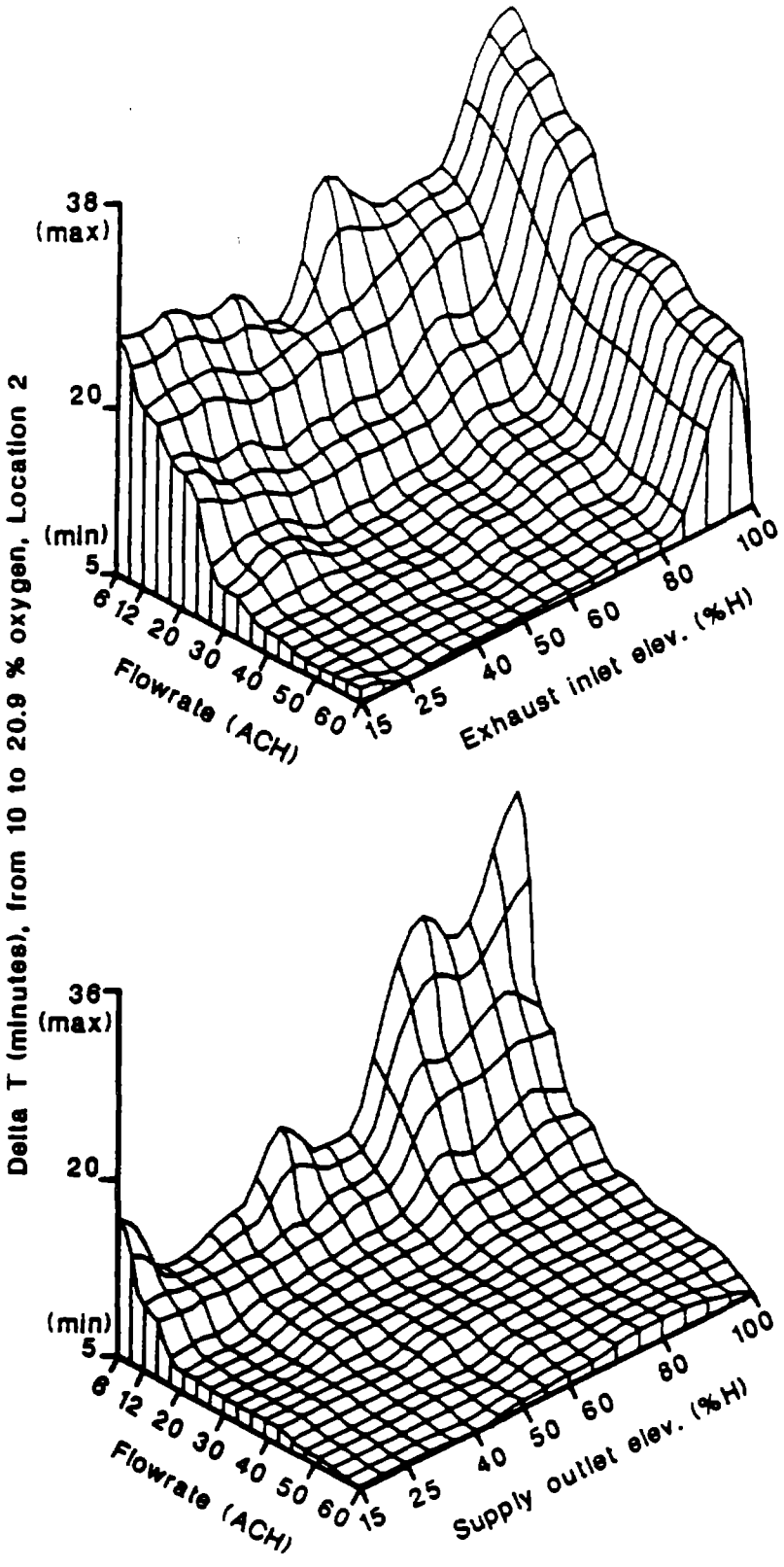

Figure 8 – Oxygen recovery time, delta T (10 to 20.9 %O_2), at Location 2 for exhaust and supply ventilation of the basic cubical CS Model A for O_2 deficiency caused by N_2 (Ref. 15).

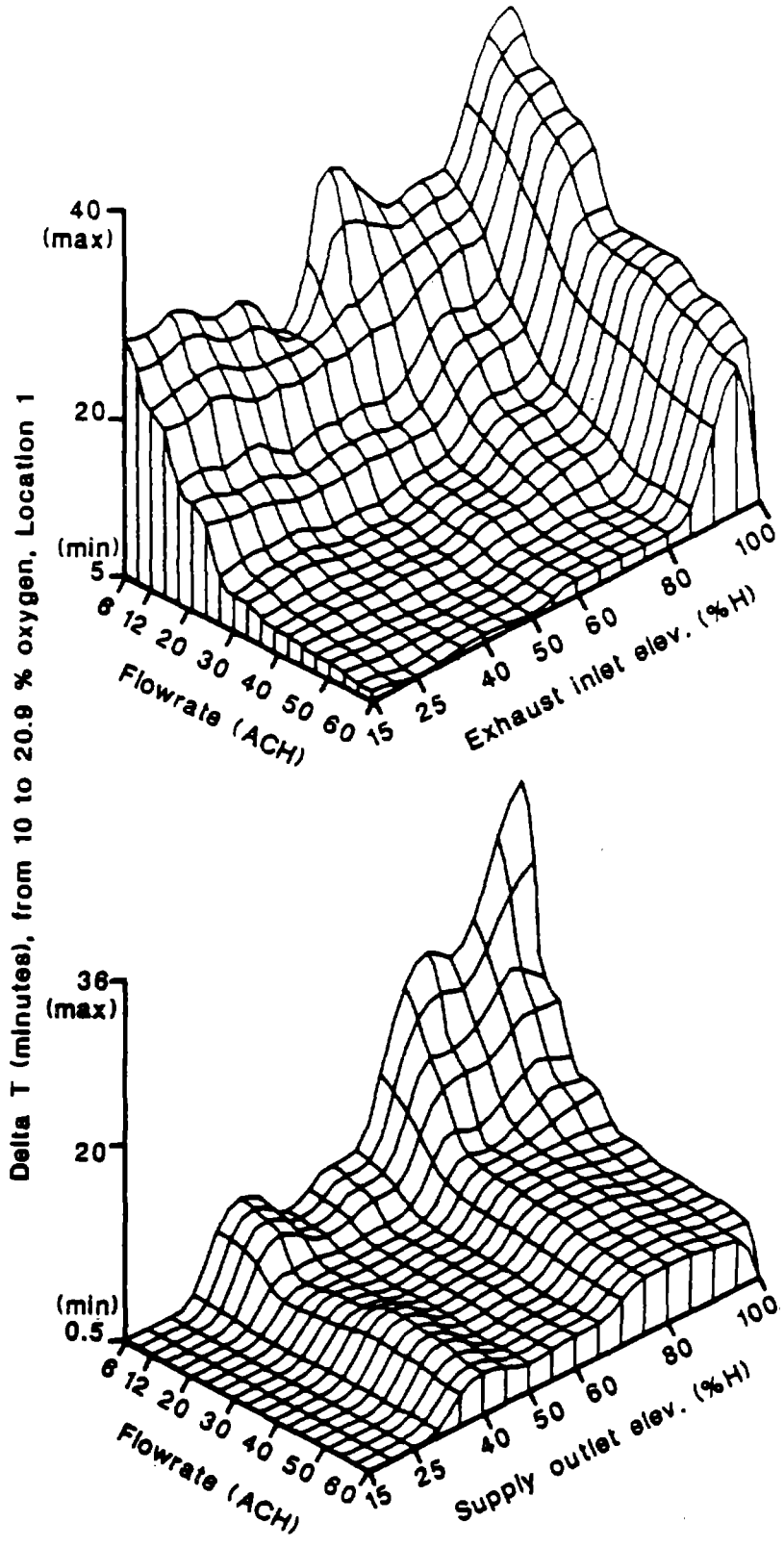

Figure 9 – Oxygen recovery time, delta T (10 to 20.9 %O_2), at Location 1 for exhaust and supply ventilation of the basic cubical CS Model A for O_2 deficiency caused by N_2 (Ref. 15).

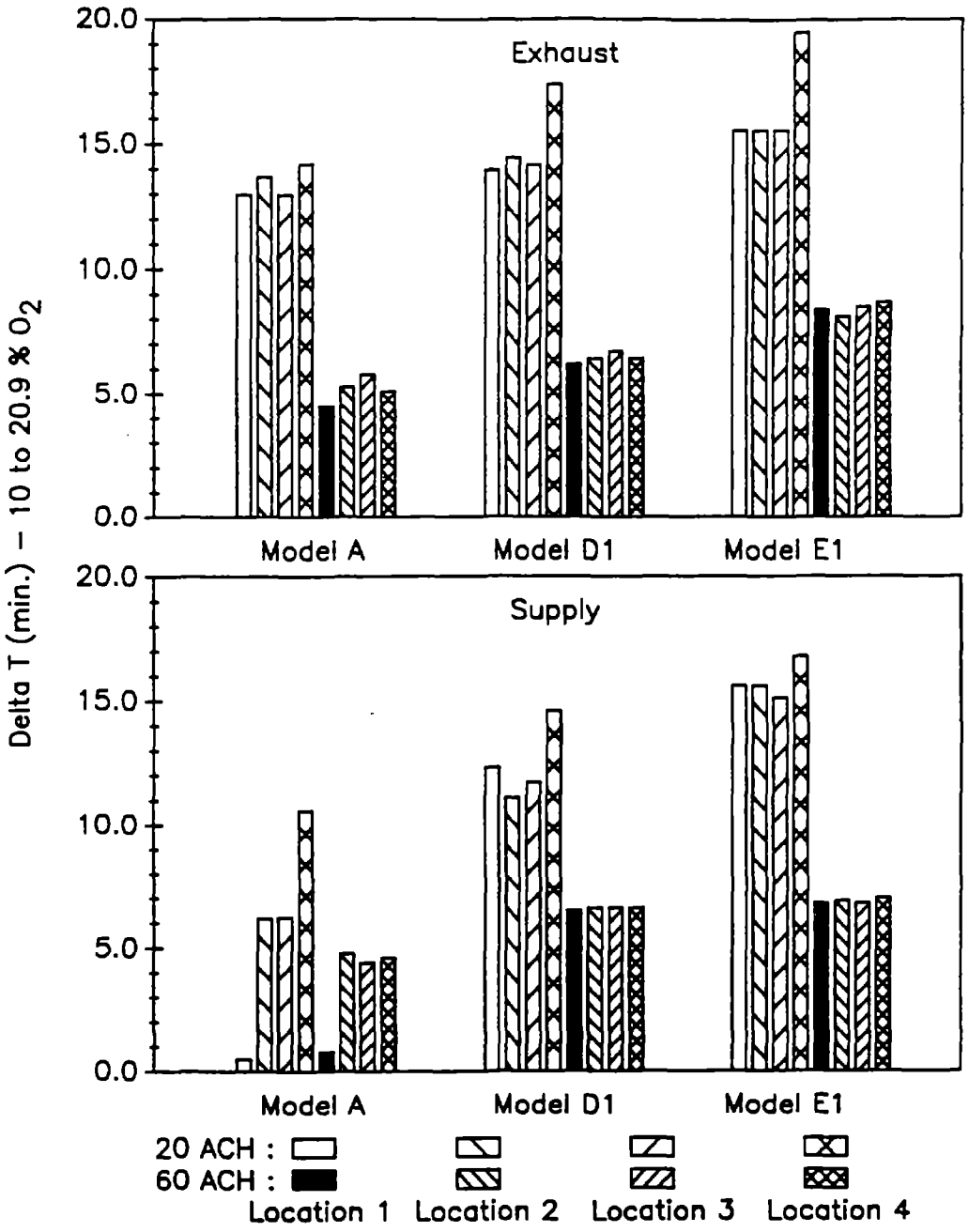

Figure 10 – Oxygen recovery times, delta T (10 to 20.9 O_2), for sideways expansion from CS Model A to CS Models D1 and E1 for O_2 deficiency caused by N_2 with exhaust and supply ventilation (I/O at 25 %H, Ref. 16).

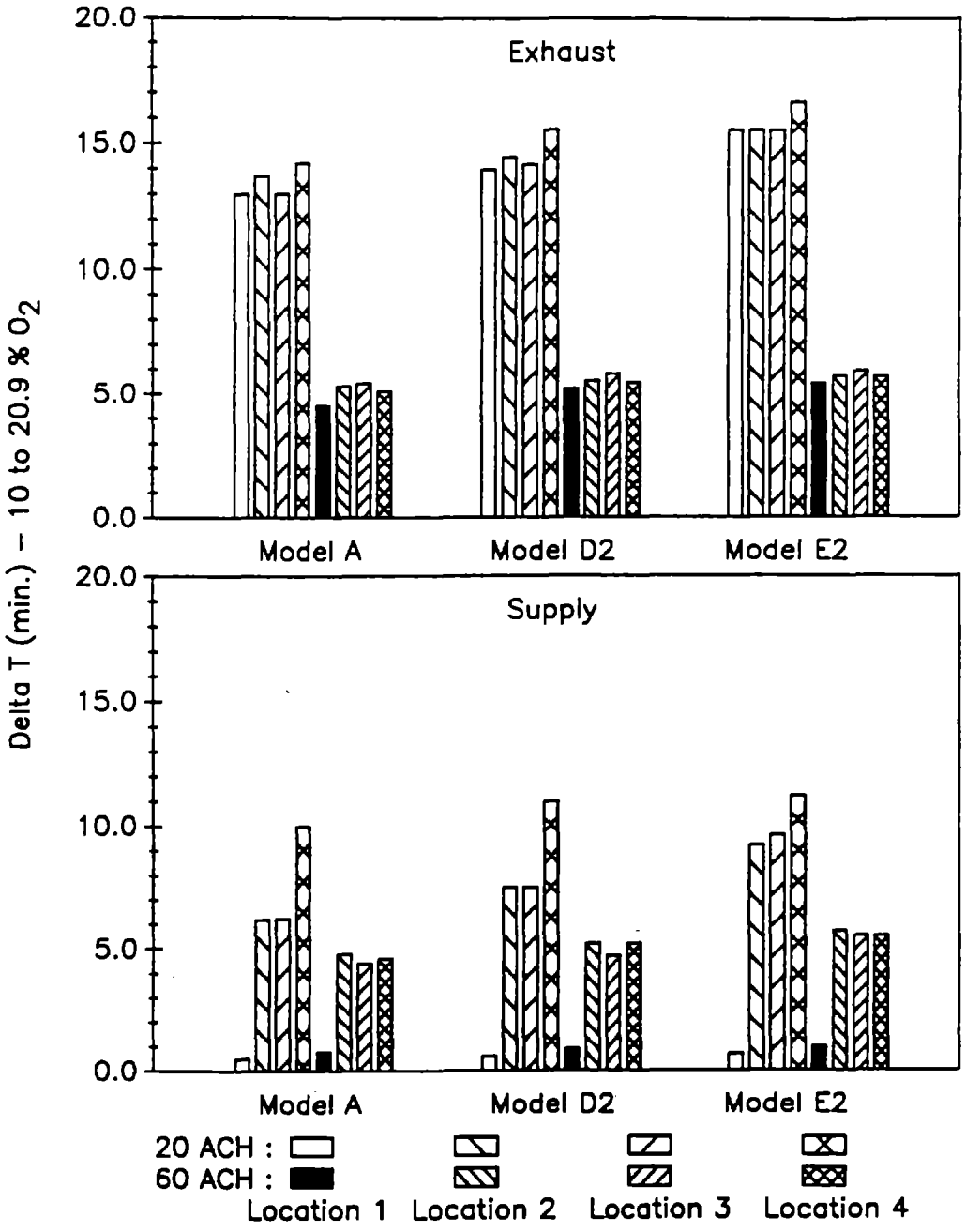

Figure 11 – Oxygen recovery times, delta T (10 to 20.9 %O_2), for depthwise expansion from CS Model A to CS Models D2 and E2 for O_2 deficiency caused by N_2 with exhaust and supply ventilation (I/O at 25 %H, Ref. 16).

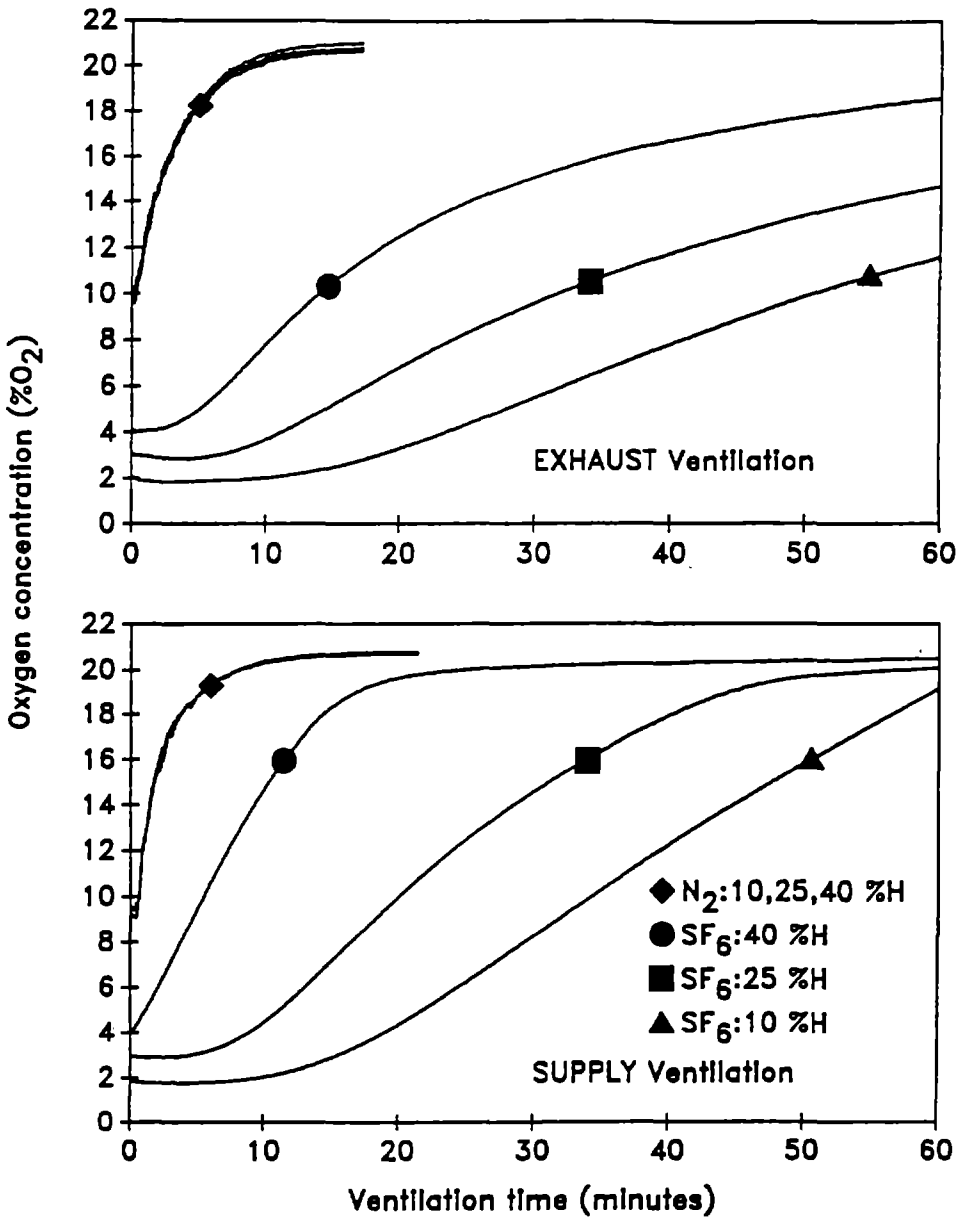

Figure 12 –Oxygen recovery for cubical CS Model Aa for O_2 deficiency caused by N_2 and SF_6 at three sampling elevations (10, 25, 40 %H), with high I/O elevation (75 %H) for exhaust and supply ventilation (20 ACH, Ref. 17).

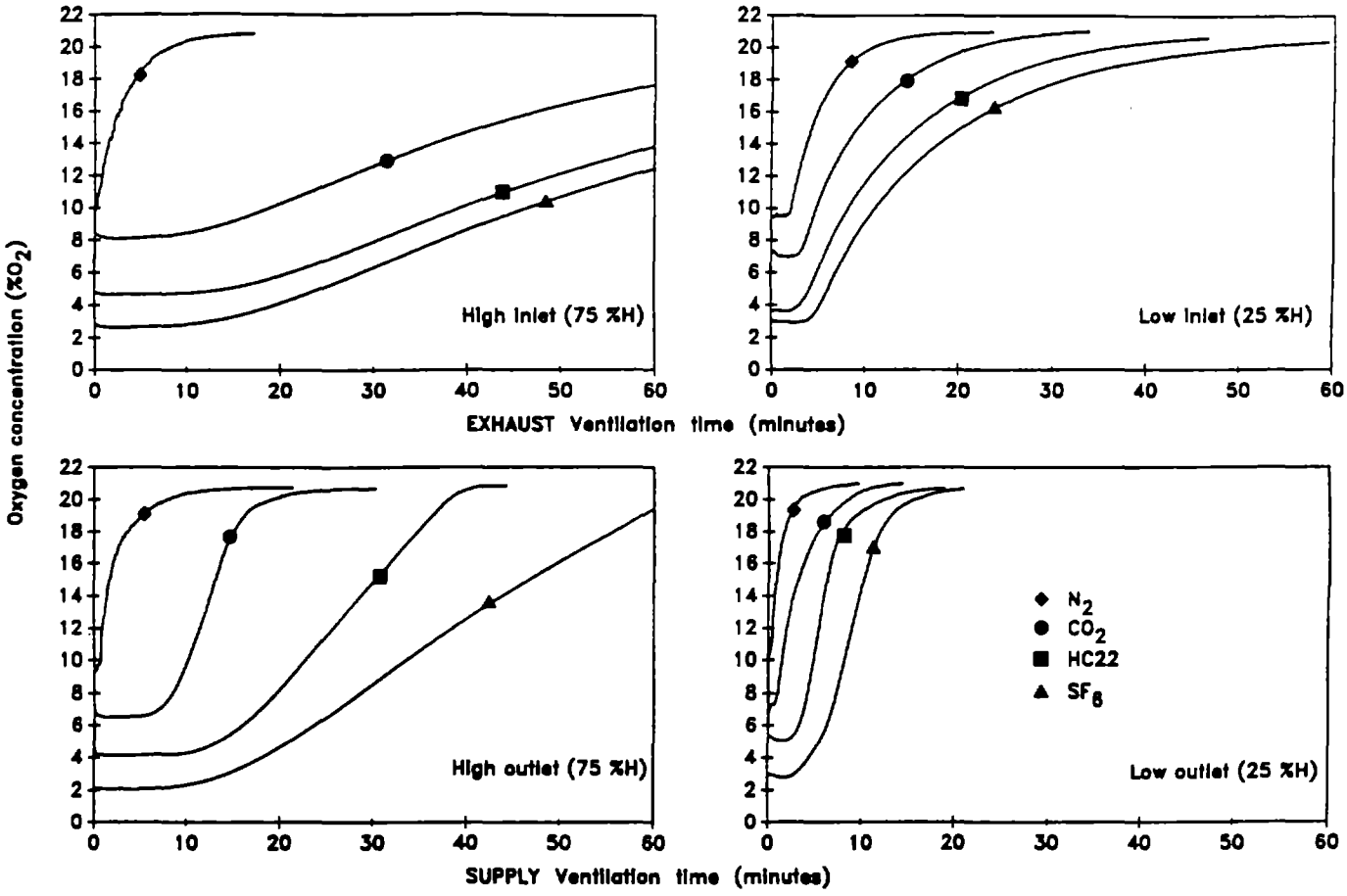

Figure 13 – Oxygen recovery for cubical CS Model Aa at the lowest sampling elevation (10 %H) for exhaust and supply ventilation for O_2 deficiency caused by heavier-than-air (HTA) contaminants (20 ACH, Ref. 17).

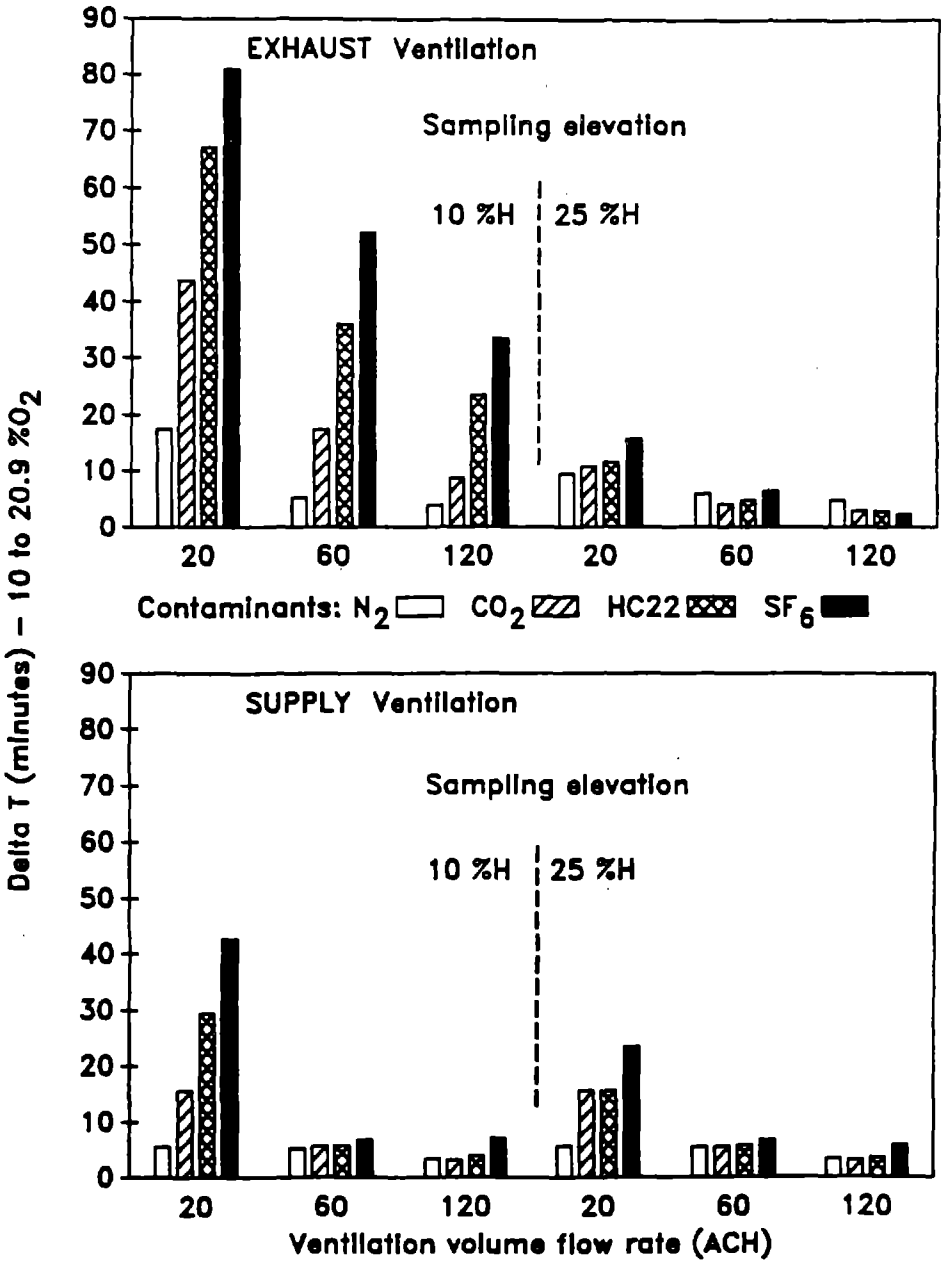

Figure 14 – Oxygen recovery times, delta T (10 to 20.9 $\%O_2$), for different ventilation volume flow rates (cubical CS Models Aa, b, c) for O_2 deficiency caused by HTA contaminants, with low I/O elevation (25 %H) exhaust and supply ventilation (Ref. 17).

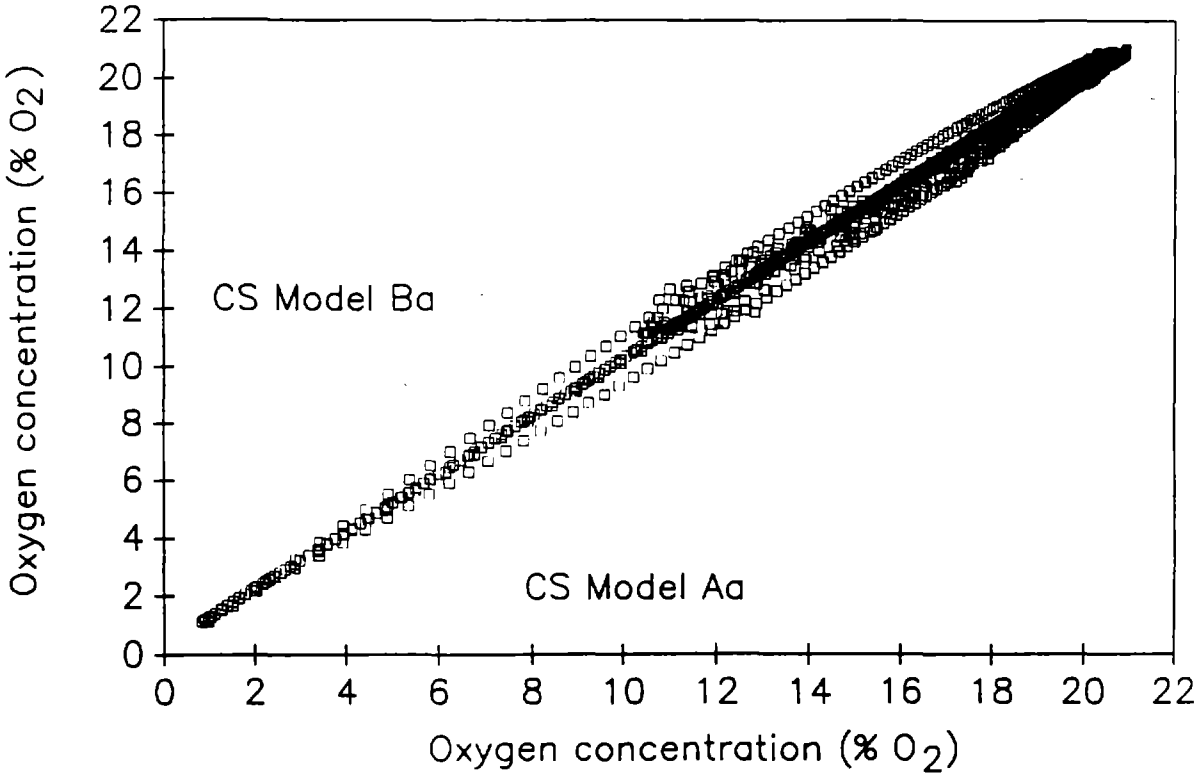

Figure 15 – Comparison of oxygen recovery data for the two geometrically-similar cubical CS Models Aa and Ba for O_2 deficiency caused by HTA contaminants (20 ACH, Ref. 17).

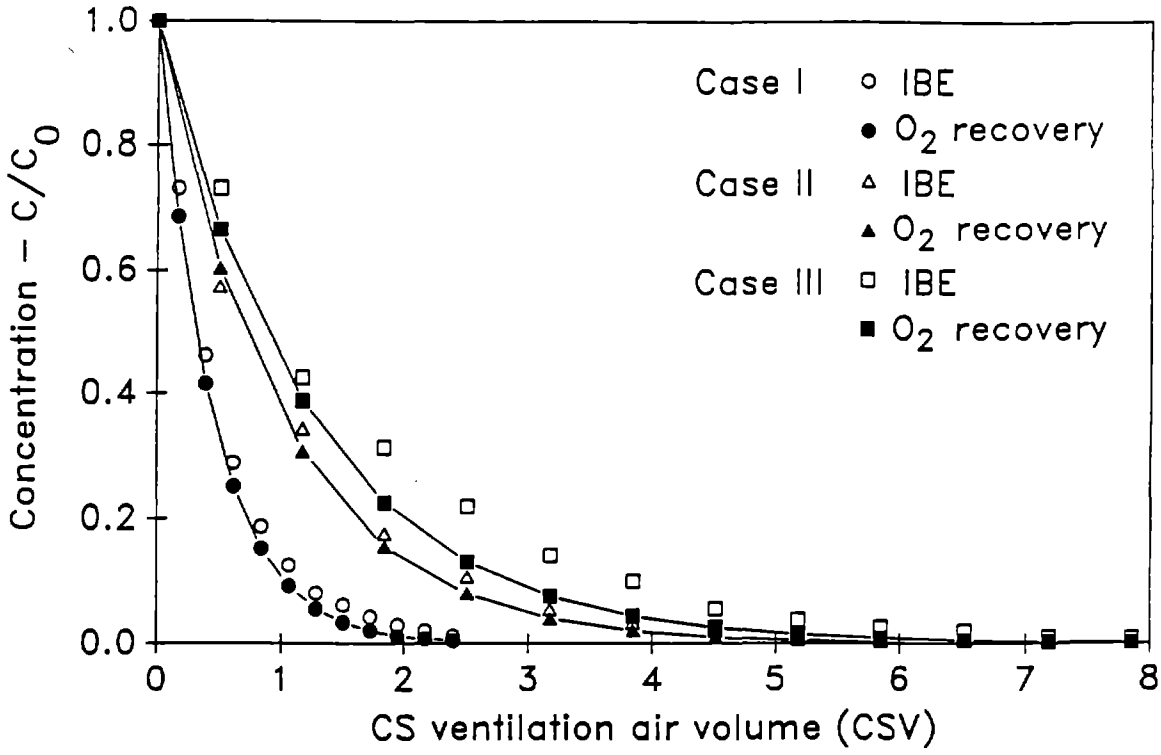

Figure 16 – Comparisons of three test-cases of contaminant reduction for simulated toxic (IBE) concentrations and for oxygen recovery from O_2 deficiency caused by N_2 (Ref. 18).

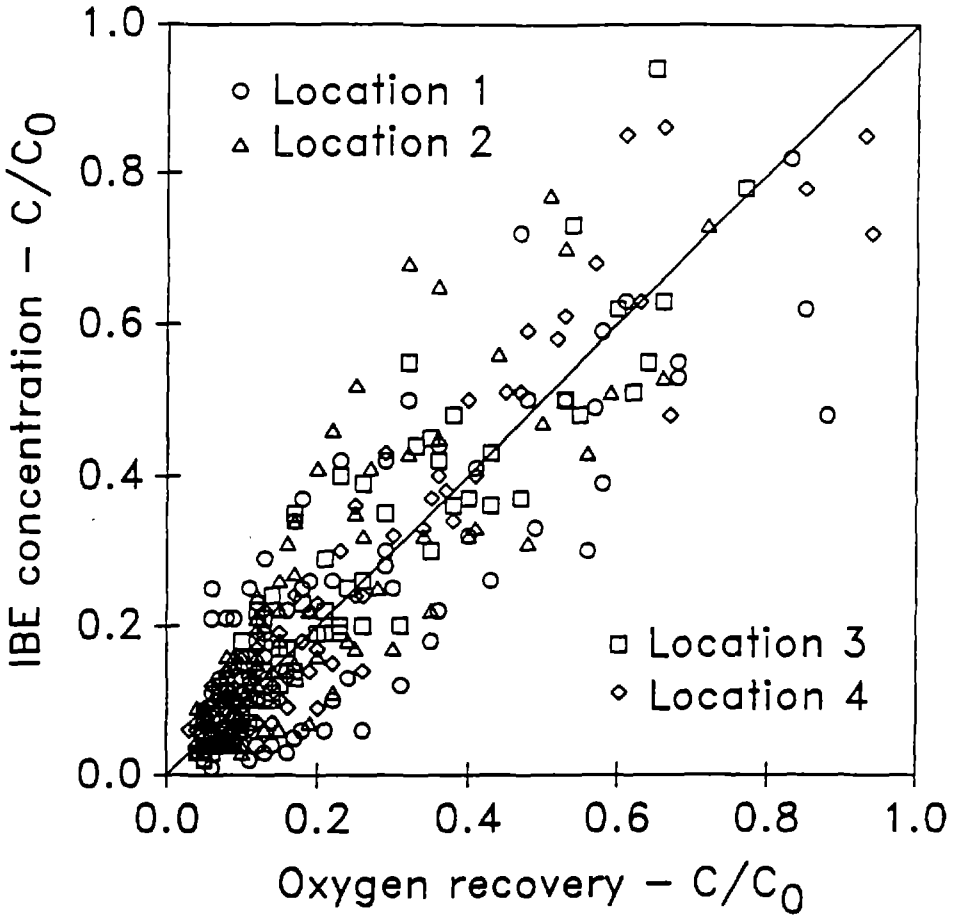

Figure 17 – Comparison of contaminant concentration data (eight test cases) for IBE reduction and for oxygen recovery from O_2 deficiency caused by N_2 (Ref. 18).

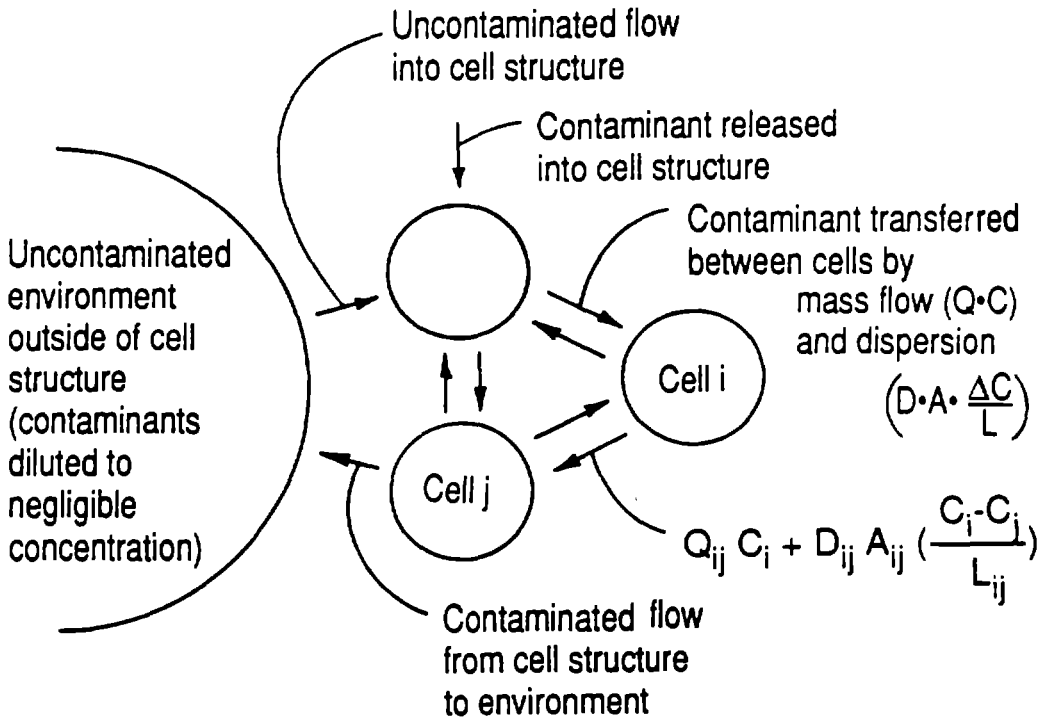

Figure 18 – Conceptual diagram of the multicellular model for contaminant dispersion and ventilation effectiveness (Ref. 19).

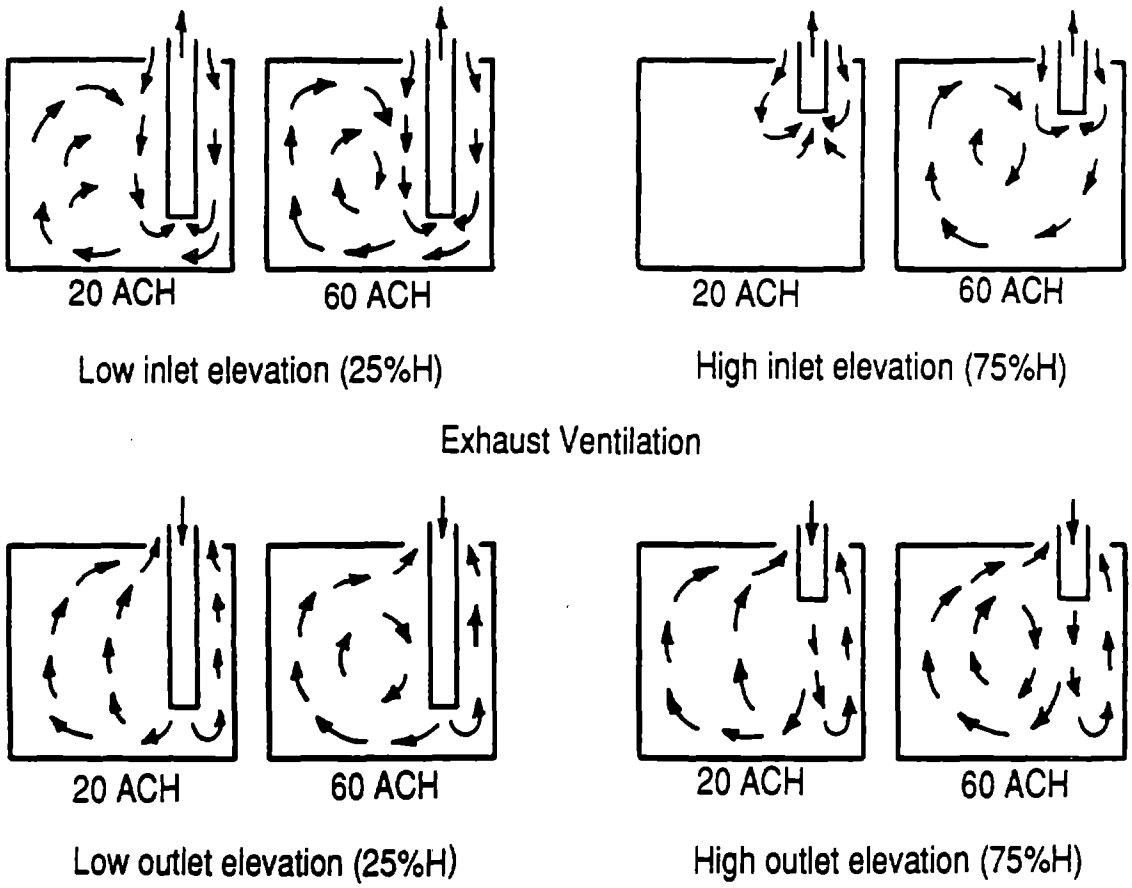

Figure 19 – Air flow patterns from tracer smoke studies of the basic cubical CS Model A (Ref. 19).

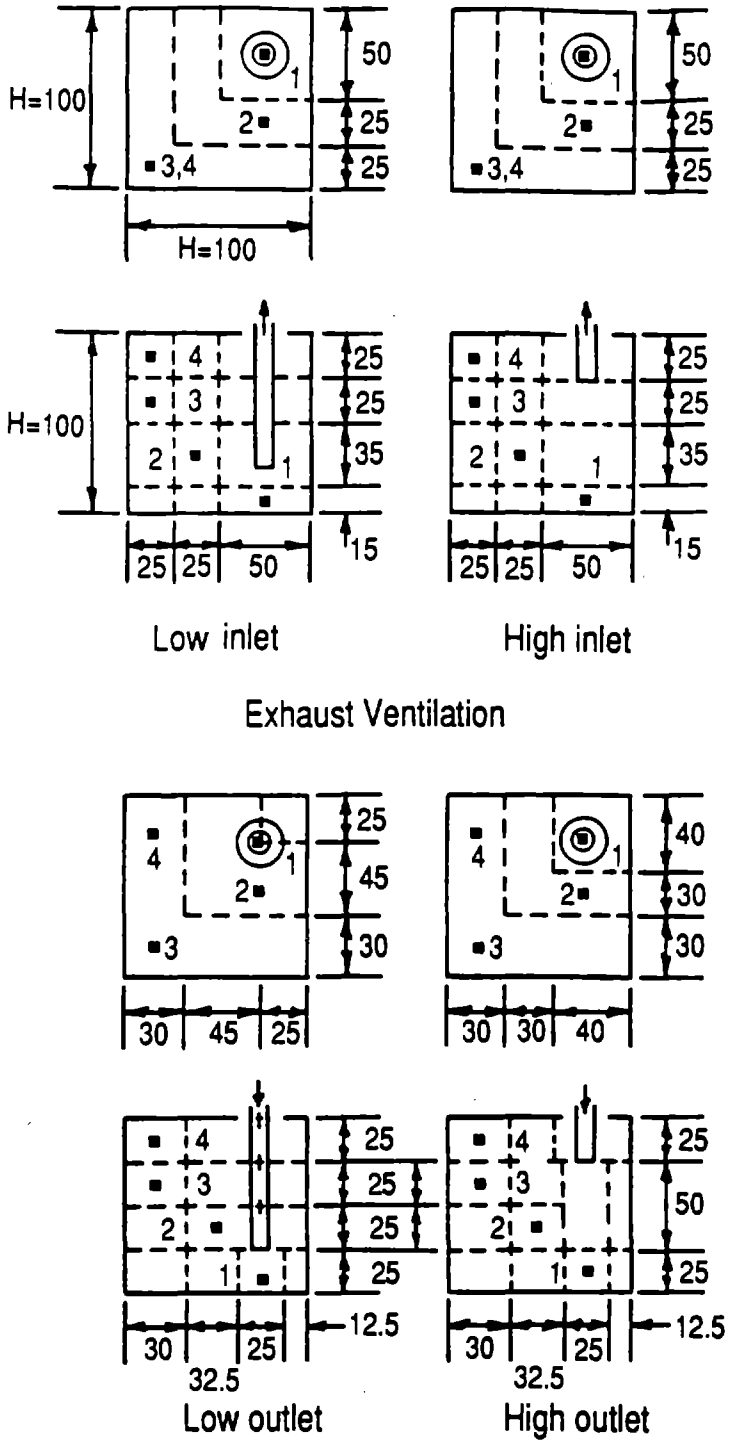

Figure 20 – Multicellular structures and sampling locations for the cubical CS Model A configurations (Ref. 19).

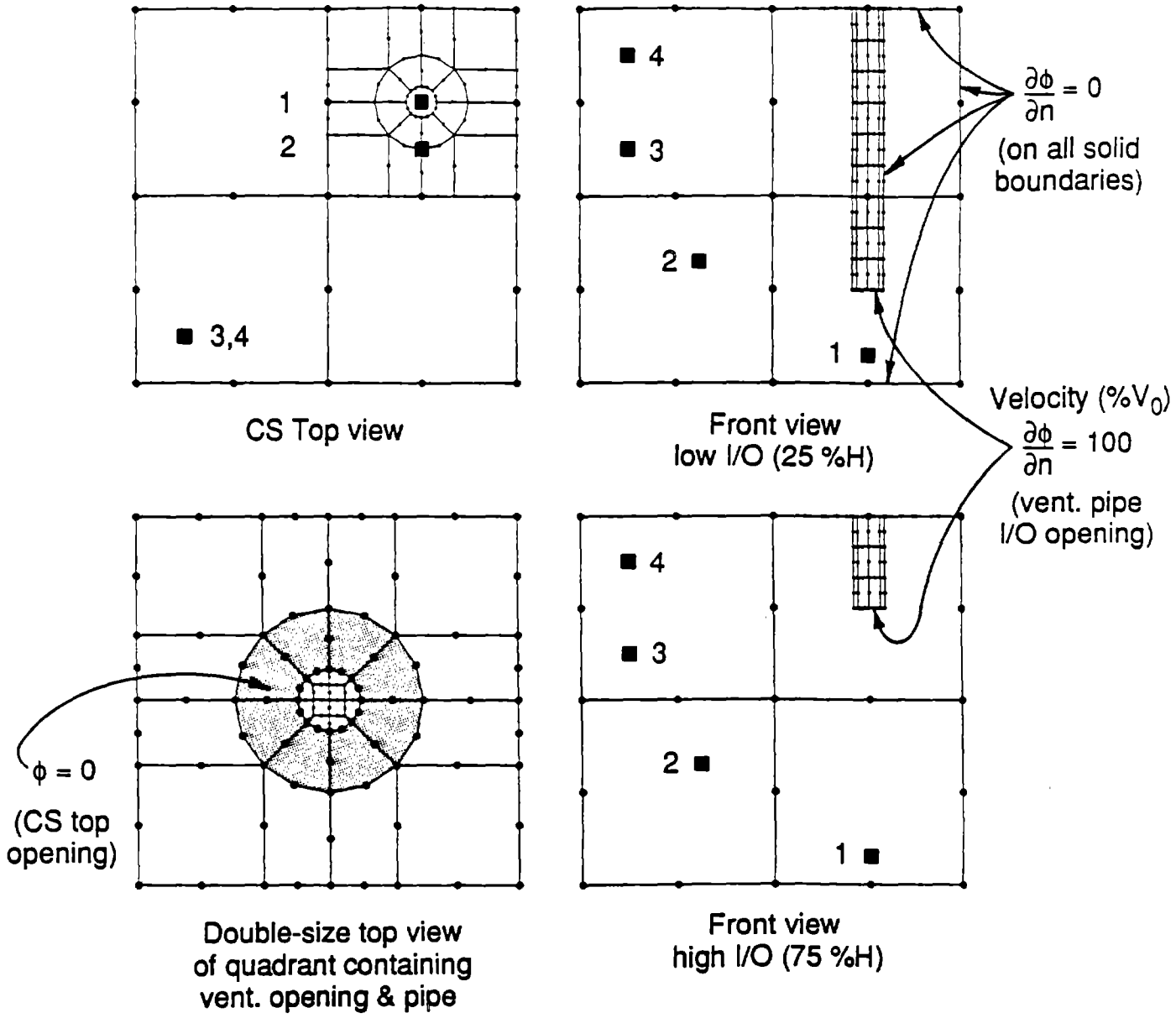

Figure 21 – BEM mesh design and boundary conditions and experimental sampling locations for cubical CS Model A (Ref. 20).

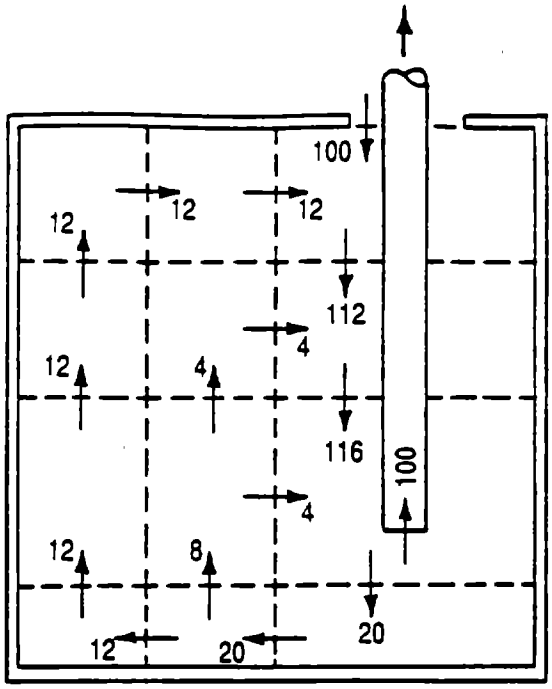

Low inlet exhaust
(25 %H, 60 ACH)

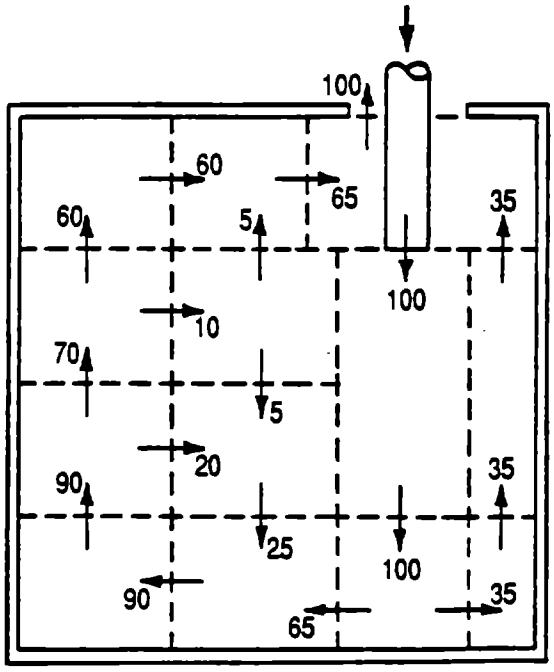

High outlet supply
(75 %H, 60 ACH)

Figure 22 – Volume (mass) flow rate approximations between cells for two test cases based upon flow patterns and velocity measurements for multicellular Model 1 (Ref. 19).

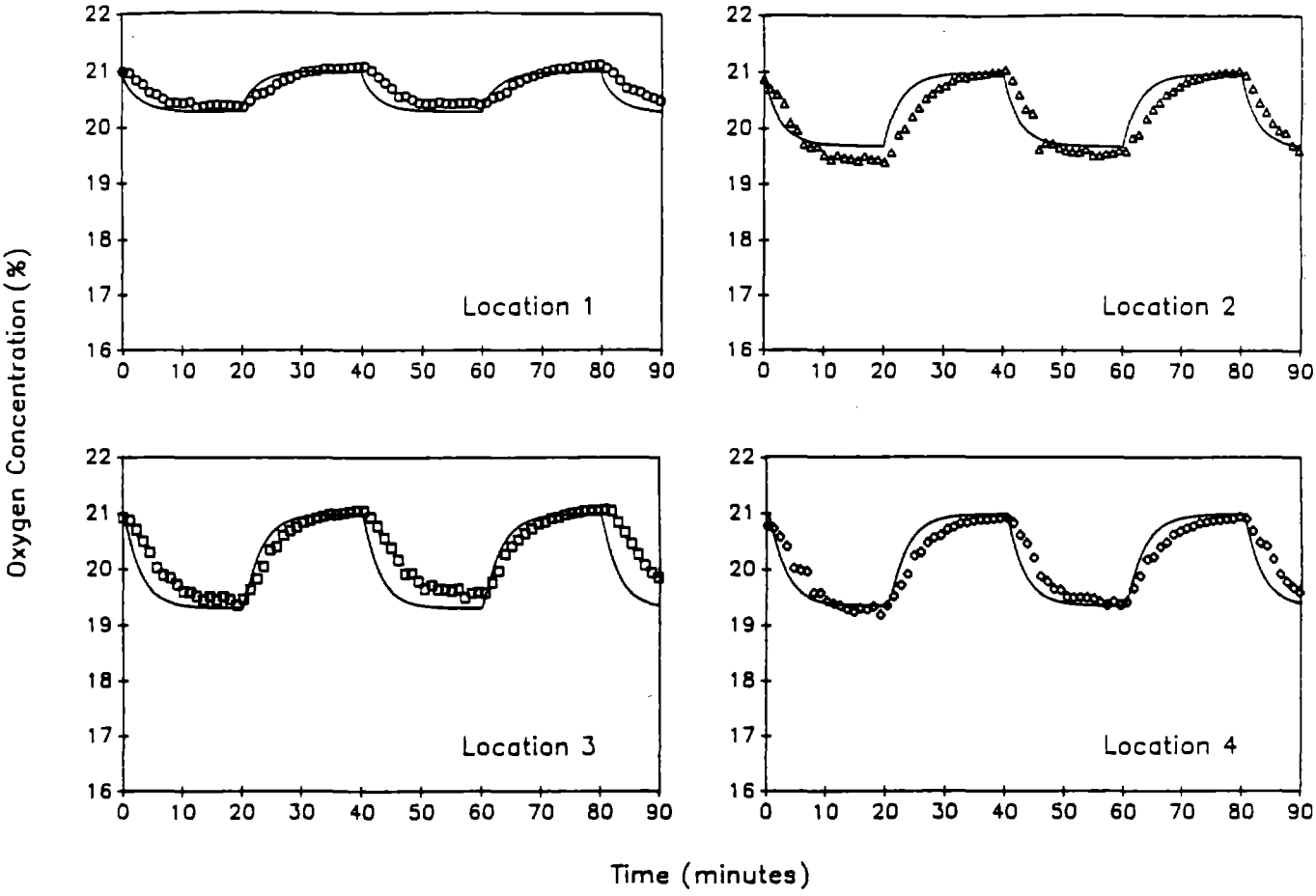

Figure 23 – Multicellular Model 1 predictions and experimental data for oxygen concentration with a variable rate of nitrogen release ("on" 10 minutes and "off" 30 minutes) for cubical CS Model A (supply ventilation, 20 ACH, 75 %H, Ref. 19).

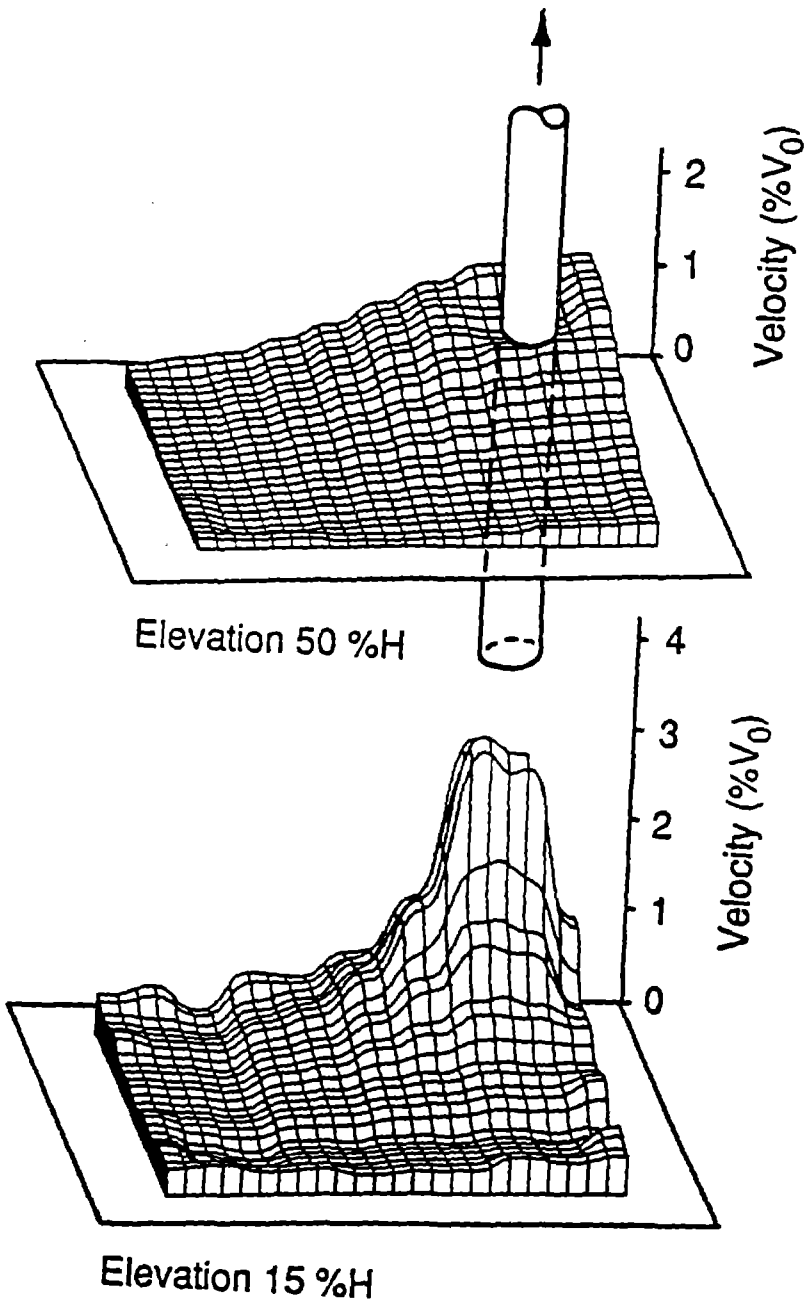

Figure 24 – Total velocity magnitude predicted by BEM at two elevations (15 and 50 %H) inside cubical CS Model A for low (25 %H) I/O elevation (Ref. 20).

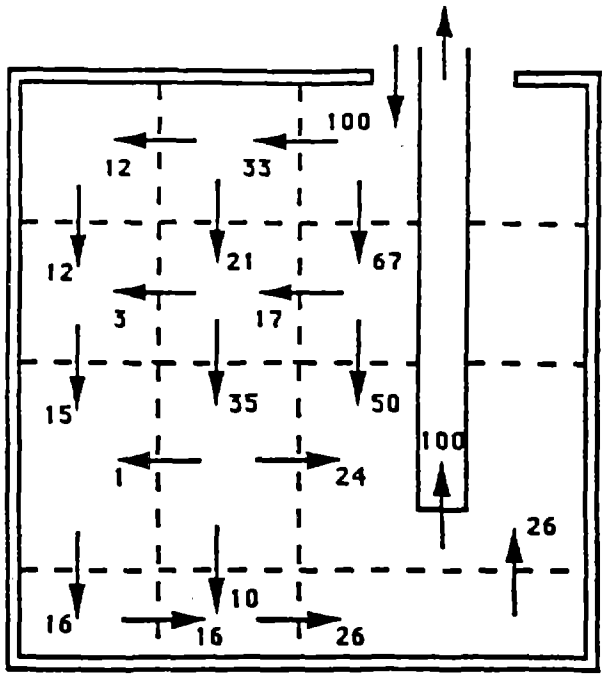

Low inlet exhaust (25 %H)

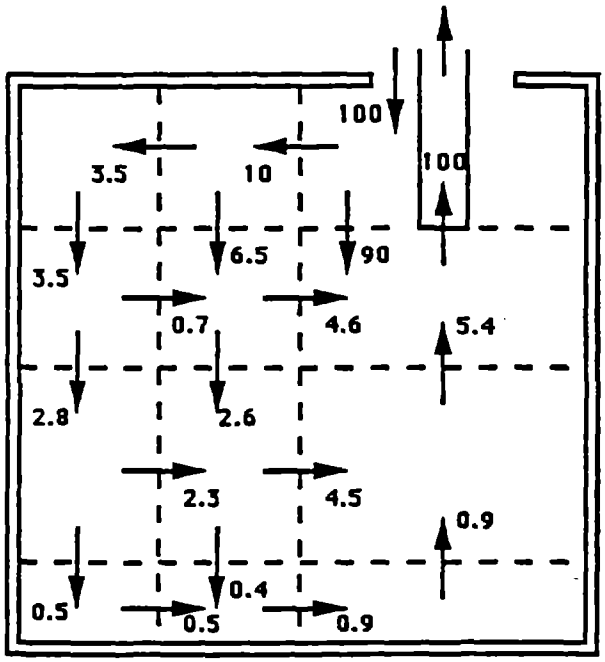

High inlet exhaust (75 %H)

Figure 25 – Volume (mass) flow rate approximations between cells for two test cases based upon velocity data predicted by BEM for multicellular Model 2 (Ref. 20).

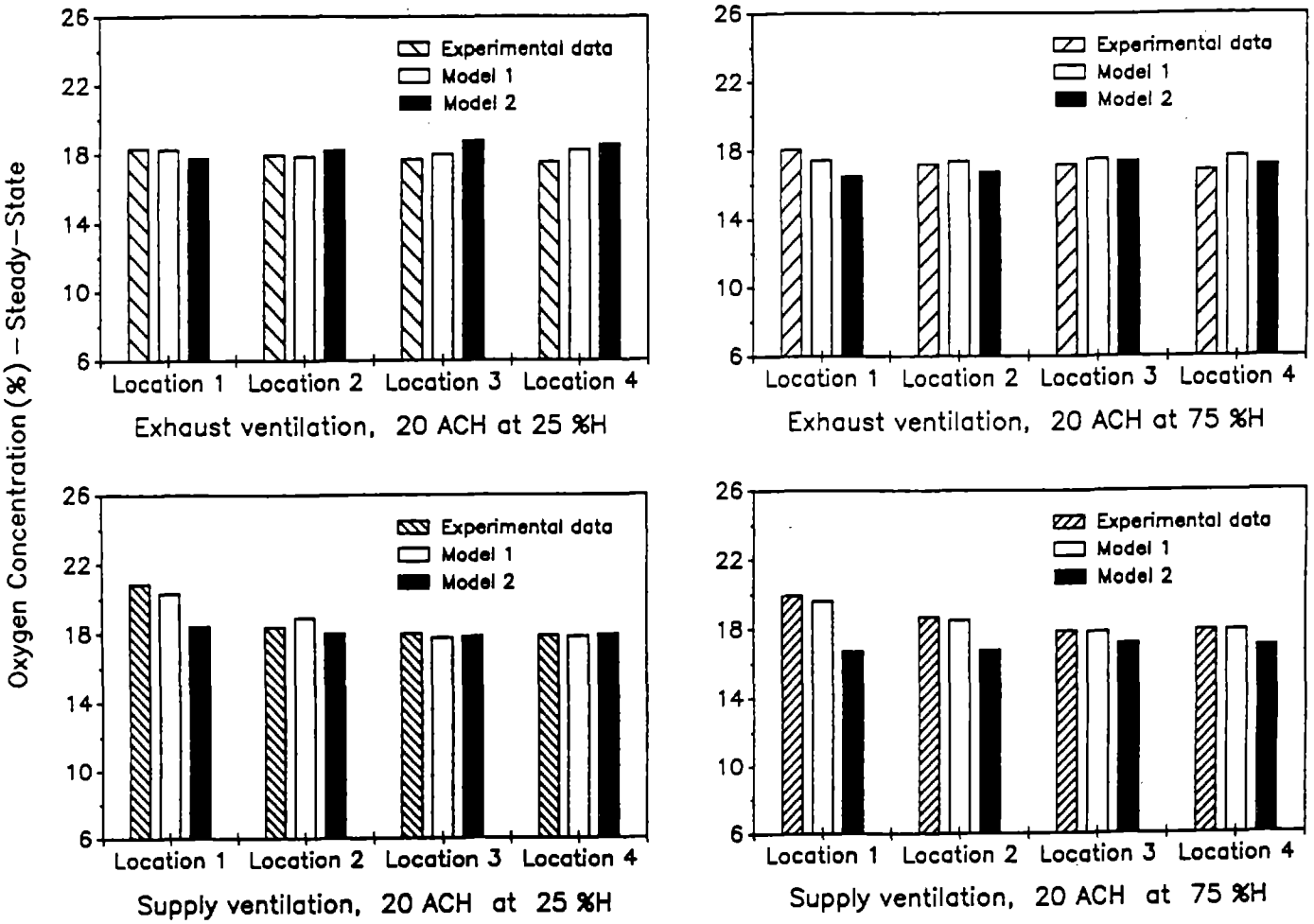

Figure 26 – Multicellular model predictions from Model 1 and Model 2 and experimental data for four test cases of steady-state oxygen concentration in cubical CS Model A (Ref. 20).

The University of Michigan
Final Inventory
Grant: 1 R01 OHO2329-01
Account: 023983

	Item	Manufacturer	Model No.	Serial No.	Tag	Acq. Date	Cost
1	Oxygen Analyzer	Enmet Corporation	ISA-40-4	1193	312194	27-Oct-87	$1,350.00
2	Photoinization Detector	Thermo Environmenta	511	2803A11375	313362	22-Sep-88	$2,944.00
3	Monitoring System	Enmet Corporation	TG-4500	126	313588	14-Nov-88	$4,000.00
						Total ==>	$8,294.00

65

65

List of Project Publications (3/27/91)

"Ventilation for Work in Confined Spaces"
Project No. 5 RO1 OH02329

In Print

1. Garrison, R.P., R. Nabar, and M. Erig: Ventilation to Eliminate Oxygen Deficiency in Confined Spaces -- Part I: A Cubical Model. Appl. Ind. Hyg. 4:1-11 (1989).

2. Garrison, R.P., and M. Erig: Ventilation to Eliminate Oxygen Deficiency in Confined Spaces -- Part II: Noncubical Models. Appl. Ind. Hyg. 4:260-268 (1989).

3. Garrison, R.P., and M. Erig: Ventilation to Eliminate Oxygen Deficiency in Confined Spaces -- Part III: Heavier-than-Air Characteristics. Appl. Occup. Environ. Hyg. 6:131-140 (1990).

4. Park, C., and R.P. Garrison: Multicellular Model for Contaminant Dispersion and Ventilation Effectiveness with Application for Oxygen Deficiency in a Confined Space. Am. Ind. Hyg. Assoc. J. 51:70-78 (1990).

Under Peer Review

5. Garrison, R.P., K. Lee, and C. Park: Contaminant Reduction by Ventilation in a Confined Space Model -- Simulated Toxic Concentrations vs. Oxygen Deficiency. Am. Ind. Hyg. Assoc. J., under peer review (1991).

6. Park, C., and R.P. Garrison: Boundary Element Method to Approximate Three-Dimensional Velocity Characteristics for a Multicellular Model of Ventilation for a Confined Space. Am. Ind. Hyg. Assoc. J., under peer review (1991).

In Preparation

7. Garrison, R.P., M. Erig, C. Park, R. Nabar, and K. Lee: Testing and Modeling of Ventilation for Confined Workplaces. Ventilation '91 -- Proceedings of the Third International Symposium on Ventilation for Contaminant Control. American Conference of Governmental Industrial Hygienists, Cincinnati, OH (will be presented in September 1991 and in press 1991/1992).